A posteriori error analysis of an HDG method for the Oseen problem

Rodolfo Araya, Manuel Solano, Patrick Vega*

CI²MA and Departamento de Ingeniería Matemática, Universidad de Concepción, Casilla 160-C, Concepción, Chile

Abstract

We propose a residual-type *a posteriori* error estimator for a hybridizable discontinuous Galerkin method applied to the Oseen problem in gradient-velocity-pressure formulation. We state reliability and local efficiency results for our estimator with respect to an error measured in the natural norms, with constants depending explicitly on the physical parameters. A weighted function technique, to control the L^2-error of the velocity, and the approximation properties of the Oswald interpolation operator are the main ingredients in the analysis. Numerical experiments in three dimensions validate our theoretical results.

Keywords: Oseen equations, hybridizable discontinuous Galerkin method, *a posteriori* error analysis
2010 MSC: 65N30

1. Introduction

The aim of this work is to introduce an *a posteriori* error estimator for a hybridizable discontinuous Galerkin (HDG) method applied to the Oseen equations. We consider the Oseen equations of a viscous and incompressible fluid at small Reynolds numbers under the action of an external body force and with prescribed velocity on the boundary of the volume containing it. The problem that we solve can be expressed as follows

$$\mathrm{L} - \nabla \boldsymbol{u} = 0 \qquad \text{in } \Omega, \tag{1.1a}$$
$$-\nabla \cdot (\nu \mathrm{L}) + \nabla p + (\boldsymbol{\beta} \cdot \nabla)\boldsymbol{u} = \boldsymbol{f} \qquad \text{in } \Omega, \tag{1.1b}$$
$$\nabla \cdot \boldsymbol{u} = 0 \qquad \text{in } \Omega, \tag{1.1c}$$
$$\boldsymbol{u} = \boldsymbol{u}_D \qquad \text{on } \Gamma, \tag{1.1d}$$
$$\int_\Omega p = 0, \tag{1.1e}$$

where $\Omega \subset \mathbb{R}^d$ $(d = 2, 3)$ is a polygonal/polyhedral domain with Lipschitz boundary Γ, $\boldsymbol{u}$ is the velocity field, p the pressure, $\nu > 0$ the effective viscosity of the fluid, $\boldsymbol{\beta} \in W^{1,\infty}(\Omega)^d$ the convective velocity of the fluid, $\boldsymbol{f} \in L^2(\Omega)^d$ an external body force and $\boldsymbol{u}_D \in H^{1/2}(\Gamma)^d$ a Dirichlet boundary data, assumed to satisfy $\int_\Gamma \boldsymbol{u}_D \cdot \boldsymbol{n} = 0$ for compatibility. We assume $\nabla \cdot \boldsymbol{\beta} = 0$ motivated by the application to the incompressible Navier–Stokes equations. In fact, one of the most common approaches to approximate the solution of the incompressible Navier–Stokes equations is to consider Picard's iteration, which consists in solving Oseen equations at every step, where the convective velocity, which is divergence free, is nothing but the velocity of the previous iteration. Now, since $\boldsymbol{\beta}$ is divergence free, it is not possible to use the standard energy argument to bound the L^2-norm of the error of $\boldsymbol{u}$ and that is why a duality argument is employed [5].

*Corresponding author
Email addresses: rodolfo.araya@udec.cl (Rodolfo Araya), msolano@ing-mat.udec.cl (Manuel Solano), pvega@ing-mat.udec.cl (Patrick Vega)

Another alternative to control this error is based on the idea of [3] (see also [22]) and assume that there is a function $\psi \in W^{1,\infty}(\Omega)$ such that $\boldsymbol{\beta} \cdot \nabla\psi \geq \frac{\|\boldsymbol{\beta}\|_{\infty,\Omega}}{\mathsf{diam}(\Omega)}$. This is satisfied, according to [3], if $\boldsymbol{\beta}$ has no closed curves and $|\boldsymbol{\beta}(\boldsymbol{x})| \neq 0$ for all $\boldsymbol{x} \in \Omega$. In this work we consider the later approach which will help us to obtain an *a posteriori* estimates for an error that includes the L^2-error of the velocity.

Oseen equations constitute an improved description of viscous and incompressible fluids at small Reynolds numbers, as compared to Stokes equations, with the partial inclusion of convective acceleration [37]. As an application of Oseen equations we can consider slow motion of small particles in a fluid, that is common in bio-mechanics [24].

Hybridization of Discontinuous Galerkin (DG) methods arises as an alternative to reduce the number of globally coupled degrees of freedom of DG methods. In the context of diffusion problems, [14] introduced a unifying framework for hybridization of DG methods, where the only globally coupled degrees of freedom are those of the numerical traces on the inter-element boundaries and the remaining unknowns are then obtained by solving local problems on each element. HDG methods have also been developed for a wide variety of problems arising from fluid mechanics, such as convection-diffusion equation [4, 9, 10, 12, 22, 31, 33, 34, 40], Stokes flow [13, 15, 16, 35], quasi-Newtonian Stokes flow [25, 26], Stokes–Darcy coupling [27], Brinkman problem [2, 21, 28], Oseen problem [5] and Navier–Stokes equations [6, 29, 36, 38, 39, 41, 42]. In the case of Oseen problem, an HDG method was proposed and analyzed in [5], for a velocity gradient-velocity-pressure formulation, obtaining optimal convergence for all the variables. Our aim is to propose an *a posteriori* error estimator for this HDG formulation.

A posteriori error analyses of DG methods have been extensively studied and a complete review is discussed in [17, 18] and the references therein. In the context of HDG methods, few contributions can be found in the literature. The first *a posteriori* error analysis of HDG methods was carried out in [17] for an LDG-H method applied to a diffusion problem. In that work, the authors proposed an efficient and reliable residual-based *a posteriori* error estimator that controls the L^2-errors of the flux $\boldsymbol{q}$ and the gradient of u. It only depends on the data oscillation and on the difference between the trace of the scalar variable u and its corresponding numerical trace. In [18], the authors provided a unified *a posteriori* error analysis for diffusion problems for a wide class of methods, including HDG, with a locally efficient and reliable error estimator that controls the L^2-norm of $\boldsymbol{q} - \widetilde{\boldsymbol{q}}_h$, where $\widetilde{\boldsymbol{q}}_h$ is any approximation of $\boldsymbol{q}$ that satisfies certain conditions (see Section 2.3.1 in [18]). Later, [7] proposed a reliable and locally efficient estimator for the convection-dominated diffusion equation, controlling the energy norm of the error. In particular, this estimator is robust with respect to the diffusion parameter. The authors also used a weighted function technique to control the L^2-error of the scalar variable. More recently, for the velocity gradient-velocity-pressure formulation of the Stokes/Brinkman problem, [2] introduced a residual-type *a posteriori* error estimator to control the L^2-error of the velocity gradient and pressure and the H^1-error of the velocity. Finally, [8] proposed an estimator for the coercive Maxwell equations.

A key ingredient in all the contributions aforementioned, is the use of the Oswald interpolation operator [20, 32], that provides a continuous approximation of a discontinuous piecewise polynomial function. Another approach consists of bounding the error in terms of the residuals by using the global inf-sup condition associated to the continuous variational formulation. In this direction, [26] proposed an error estimator for an augmented HDG method applied to a class of quasi-Newtonian Stokes equations in velocity gradient-pseudostress-velocity formulation and [28] employed similar techniques to derive an error estimator for an HDG method applied to the Brinkman problem in pseudostress-velocity formulation. As another contribution on adaptivity for HDG methods, the first fully computable a posteriori error bounds for HDG methods have been recently presented in [1].

The main contribution of our work is to propose and analyse an *a posteriori* estimator of an HDG method for Oseen equations, where the unknowns are de velocity, pressure and the gradient of the velocity. We propose a reliable and locally efficient residual-based *a posteriori* error estimator for the Oseen problem, constructed in terms of an element-by-element postprocessing of the velocity having superconvergence properties, using the Oswald interpolation operator and a weighted function technique to control the L^2-norm of the velocity. In addition, all the constants in the estimates are written explicitly in terms of the physical parameters $\boldsymbol{\beta}$ and ν.

The paper is organized as follows. In Section 2, we present the HDG method, notation and basic definitions. In Section 3, we introduce our *a posteriori* error estimator and state the main results about it. Finally, in Section 4 we show numerical evidence, in dimension three, that validates our theoretical results and an application to steady-state incompressible Navier–Stokes equations.

2. The method

2.1. Notation

Let $\{\mathcal{T}_h\}_{h>0}$ be a shape-regular family of conforming simplicial triangulations of the domain $\overline{\Omega}$. Let h_S be the diameter of an element or face S, as appropriate. We denote by $\mathcal{E}_h^i$ and $\mathcal{E}_h^\partial$ the set of interior and boundary faces, respectively, and sets $\mathcal{E}_h := \mathcal{E}_h^i \cup \mathcal{E}_h^\partial$, $\partial\mathcal{T}_h := \{\partial K : K \in \mathcal{T}_h\}$, $\omega_e := \{K \in \mathcal{T}_h : e \subset \partial K\}$. We will use bold and roman letters to denote vector- and tensor-valued variables, respectively. For a tensor-valued function G and a vector-valued function $\boldsymbol{v}$, we define

$$[\![\mathrm{G}]\!] = \begin{cases} \mathrm{G}^-\boldsymbol{n}^- + \mathrm{G}^+\boldsymbol{n}^+, & e \in \mathcal{E}_h \setminus \mathcal{E}_h^\partial \\ \mathbf{0}, & e \in \mathcal{E}_h^\partial \end{cases} \quad \text{and} \quad [\![\boldsymbol{v}]\!] = \begin{cases} \boldsymbol{v}^+ - \boldsymbol{v}^-, & e \in \mathcal{E}_h \setminus \mathcal{E}_h^\partial \\ \boldsymbol{v} - \boldsymbol{u}_D, & e \in \mathcal{E}_h^\partial \end{cases},$$

where $\boldsymbol{n}$ denotes the outward unit normal vector to ∂K. We use the notation $(\cdot,\cdot)_K$ and $\langle\cdot,\cdot\rangle_e$ for the L^2-inner product on $K \in \mathcal{T}_h$ and $e \in \mathcal{E}_h$, respectively, and define $(\cdot,\cdot)_D := \sum_{K\in D}(\cdot,\cdot)_K$ and $\langle\cdot,\cdot\rangle_D := \sum_{e\in D}\langle\cdot,\cdot\rangle_e$, where $D \subseteq \mathcal{T}_h$ or $D \subseteq \mathcal{E}_h$, as appropriate. Let us also define

$$|\!|\!|\boldsymbol{v}|\!|\!|_K := \left(\frac{\|\boldsymbol{\beta}\|_{\infty,\Omega}}{\mathsf{diam}(\Omega)}\|\boldsymbol{v}\|_{0,K}^2 + \nu\|\nabla\boldsymbol{v}\|_{0,K}^2\right)^{1/2},$$

and $|\!|\!|\cdot|\!|\!|_D := \left(\sum_{K\in D} |\!|\!|\cdot|\!|\!|_K\right)^{1/2}$, where $\|\cdot\|_{0,K}$ is induced by $(\cdot,\cdot)_K$. At last, $\mathbb{P}_k(S)$ will denote the space of polynomials of total degree no greater than $k \in \mathbb{N}$, with S being a simplex or a face as appropriate.

In what follows, we will use $a \preceq b$ to denote $a \leq Cb$, where C is a generic positive constant independent of h and the physical parameters of the equation.

2.2. An HDG method for the Oseen problem

Let us consider the finite element spaces

$$\mathrm{G}_h := \{\mathrm{G} \in L^2(\mathcal{T}_h)^{d\times d} : \mathrm{G}|_K \in \mathbb{P}_k(K)^{d\times d} \quad \forall K \in \mathcal{T}_h\}, \tag{2.1a}$$

$$\boldsymbol{V}_h := \{\boldsymbol{v} \in L^2(\mathcal{T}_h)^d : \boldsymbol{v}|_K \in \mathbb{P}_k(K)^d \quad \forall K \in \mathcal{T}_h\}, \tag{2.1b}$$

$$P_h := \{w \in L^2(\mathcal{T}_h) : w|_T \in \mathbb{P}_k(K) \quad \forall K \in \mathcal{T}_h\}, \tag{2.1c}$$

$$\boldsymbol{M}_h := \{\boldsymbol{\mu} \in L^2(\mathcal{E}_h)^d : \boldsymbol{\mu}|_e \in \mathbb{P}_k(e)^d \quad \forall e \in \mathcal{E}_h\} \tag{2.1d}$$

and the HDG formulation, introduced in [5], for the Oseen problem (1.1): *Find* $(\mathrm{L}_h, \boldsymbol{u}_h, p_h, \widehat{\boldsymbol{u}}_h) \in \mathrm{G}_h \times \boldsymbol{V}_h \times P_h \times \boldsymbol{M}_h$ *such that*

$$(\mathrm{L}_h, \mathrm{G})_{\mathcal{T}_h} + (\boldsymbol{u}_h, \nabla\cdot\mathrm{G})_{\mathcal{T}_h} - \langle\widehat{\boldsymbol{u}}_h, \mathrm{G}\boldsymbol{n}\rangle_{\partial\mathcal{T}_h} = 0, \tag{2.2a}$$

$$(\nu\mathrm{L}_h, \nabla\boldsymbol{v})_{\mathcal{T}_h} - (\boldsymbol{u}_h\otimes\boldsymbol{\beta}, \nabla\boldsymbol{v})_{\mathcal{T}_h} - (p_h, \nabla\cdot\boldsymbol{v})_{\mathcal{T}_h} - \langle\nu\widehat{\mathrm{L}}_h\boldsymbol{n} - (\widehat{\boldsymbol{u}_h\otimes\boldsymbol{\beta}})\boldsymbol{n} - \widehat{p}_h\boldsymbol{n}, \boldsymbol{v}\rangle_{\partial\mathcal{T}_h} = (\boldsymbol{f}, \boldsymbol{v})_{\mathcal{T}_h}, \tag{2.2b}$$

$$-(\boldsymbol{u}_h, \nabla q)_{\mathcal{T}_h} + \langle\widehat{\boldsymbol{u}}_h\cdot\boldsymbol{n}, q\rangle_{\partial\mathcal{T}_h} = 0, \tag{2.2c}$$

$$\langle\widehat{\boldsymbol{u}}_h, \boldsymbol{\mu}\rangle_\Gamma = \langle\boldsymbol{u}_D, \boldsymbol{\mu}\rangle_\Gamma, \tag{2.2d}$$

$$\langle\nu\widehat{\mathrm{L}}_h\boldsymbol{n} - (\widehat{\boldsymbol{u}_h\otimes\boldsymbol{\beta}})\boldsymbol{n} - \widehat{p}_h\boldsymbol{n}, \boldsymbol{\mu}\rangle_{\partial\mathcal{T}_h\setminus\Gamma} = 0, \tag{2.2e}$$

$$(p_h, 1)_\Omega = 0, \tag{2.2f}$$

for all $(\mathrm{G}, \boldsymbol{v}, q, \boldsymbol{\mu}) \in \mathrm{G}_h \times \boldsymbol{V}_h \times P_h \times \boldsymbol{M}_h$. To complete the definition of the scheme, we specify the numerical trace $\nu\widehat{\mathrm{L}}_h\boldsymbol{n} - (\widehat{\boldsymbol{u}_h \otimes \boldsymbol{\beta}})\boldsymbol{n} - \widehat{p}_h\boldsymbol{n} := \nu\mathrm{L}_h\boldsymbol{n} - (\widehat{\boldsymbol{u}}_h \otimes \boldsymbol{\beta})\boldsymbol{n} - p_h\boldsymbol{n} - \nu\tau(\boldsymbol{u}_h - \widehat{\boldsymbol{u}}_h)$ on $\partial\mathcal{T}_h$, where τ is a positive stabilization function on $\partial\mathcal{T}_h$ that satisfies

$$\min_{\boldsymbol{x}\in\partial K}\left(\nu\tau - \frac{1}{2}\boldsymbol{\beta}\cdot\boldsymbol{n}\right) > 0 \quad \forall K \in \mathcal{T}_h. \tag{2.3}$$

As it is shown in [5], this scheme is well-posed and, if L, $\boldsymbol{u}$ and p have enough regularity, the approximate solution satisfies

$$\|\mathrm{L} - \mathrm{L}_h\|_{0,\mathcal{T}_h} + \|\boldsymbol{u} - \boldsymbol{u}_h\|_{0,\mathcal{T}_h} + \|p - p_h\|_{0,\mathcal{T}_h} \leq c_{\nu,\boldsymbol{\beta}} \sum_{K\in\mathcal{T}_h} h_K^{k+1}\Theta_K, \tag{2.4a}$$

where $c_{\nu,\boldsymbol{\beta}} > 0$ is a constant depending on ν and $\boldsymbol{\beta}$ and $\Theta_K := |\mathrm{L}|_{k+1} + |\boldsymbol{u}|_{k+1} + |\nabla\cdot(\nu\mathrm{L} - p\mathrm{I})|_{k,K} + |p|_{k+1,K}$.

2.3. Local postprocessing of the velocity

Our a posteriori error estimator will be defined in terms of a local postprocessing $\boldsymbol{u}_h^*$ of $\boldsymbol{u}_h$ that approximates $\boldsymbol{u}$ with enhanced accuracy. In our case, we construct $\boldsymbol{u}_h^*$ as follows. We seek $\boldsymbol{u}_h^* \in \boldsymbol{V}_h^* := \{\boldsymbol{w} \in L^2(\Omega)^d : \boldsymbol{w}|_K \in \mathbb{P}_{k+1}(K)^d\ \forall K \in \mathcal{T}_h\}$ such that, for all $K \in \mathcal{T}_h$, it satisfies

$$(\nabla\boldsymbol{u}_h^*, \nabla\boldsymbol{w})_K = (\mathrm{L}_h, \nabla\boldsymbol{w})_K \quad \forall\boldsymbol{w} \in \mathbb{P}_{k+1}(K)^d \tag{2.5a}$$

$$(\boldsymbol{u}_h^*, \boldsymbol{w})_K = (\boldsymbol{u}_h, \boldsymbol{w})_K \qquad \forall\boldsymbol{w} \in \mathbb{P}_0(K)^d. \tag{2.5b}$$

It's straightforward to see that $\boldsymbol{u}_h^*$ is well defined. Moreover, this new approximation has superconvergence properties (see [2]).

3. A posteriori error analysis

3.1. Preliminaries

To start, we provide auxiliary results needed to prove the reliability and efficiency of the error estimator. They were also considered in the *a posteriori* error estimates for the Brinkman problem [2] and we state them here in order to make the manuscript self-contained.

Let us consider the Clément interpolation operator $\mathcal{C}_h : L^1(\Omega) \to V_h^{1,c} \cap H_0^1(\Omega)$ introduced in [11]:

$$\mathcal{C}_h w := \sum_{z\in\mathcal{N}_h^i}\left(\frac{1}{|\Omega_z|}\int_{\Omega_z} w \ \mathrm{d}x\right)\phi_z,$$

where ϕ_z is the $\mathbb{P}_1$ nodal basis functions associated to the interior vertex z, $\Omega_z := \mathrm{supp}\ \phi_z$, $\mathcal{N}_h^i$ the set of all interior vertices and $V_h^{1,c} := \{w \in \mathcal{C}(\Omega) : w|_K \in \mathbb{P}_1(K),\ K \in \mathcal{T}_h\}$.

Lemma 3.1. *For any* $K \in \mathcal{T}_h$, $e \in \mathcal{E}_h^i$, $0 \leq m \leq 1$ *and* $w \in H_0^1(\Omega)$, *there hold:*

$$\|\mathcal{C}_h w\|_{m,\Omega} \preceq \|w\|_{m,\Omega}, \quad \|w - \mathcal{C}_h w\|_{0,K} \preceq \theta_K |||w|||_{1,\Delta_K} \quad \textit{and} \quad \|w - \mathcal{C}_h w\|_{0,e} \preceq \nu^{-1/4}\theta_e^{1/2} |||w|||_{1,\Delta_e},$$

where $\theta_S := \min\{h_S\nu^{-1/2}, \mathsf{diam}(\Omega)^{1/2}\|\boldsymbol{\beta}\|_{\infty,\Omega}^{-1/2}\}$, *with* S *an element* $K \in \mathcal{T}_h$ *or a face* $e \in \mathcal{E}_h$, $\Delta_K := \{K' \in \mathcal{T}_h : \overline{K'} \cap \overline{K} \neq \emptyset\}$ *and* $\Delta_e := \{K' \in \mathcal{T}_h : \overline{K'} \cap \overline{e} \neq \emptyset\}$.

Proof. See Lemma 3.2 in [44]. □

The next result gives an approximation property of the Oswald interpolation operator, that approximates $\boldsymbol{w} \in \boldsymbol{V}_h$ by a continuous function $\widetilde{\boldsymbol{w}} \in \boldsymbol{V}_h$.

Lemma 3.2. *Let D^γ be the row-wise gradient or identity operator (for $|\gamma| = 1$ or $|\gamma| = 0$, respectively). For any $\boldsymbol{w}_h \in \boldsymbol{V}_h^*$ and any multi-index γ with $|\gamma| = 0, 1$ the following approximation result holds: Let $\boldsymbol{g}$ be the restriction to Γ of a function in $\boldsymbol{V}_h^* \cap H^1(\Omega)^d$. Then, there exists a function $\widetilde{\boldsymbol{w}}_h \in \boldsymbol{V}_h^* \cap H^1(\Omega)^d$ satisfying $\widetilde{\boldsymbol{w}}_h|_\Gamma = \boldsymbol{g}$ and*

$$\sum_{K\in\mathcal{T}_h} \|D^\gamma(\boldsymbol{w}_h - \widetilde{\boldsymbol{w}}_h)\|_{0,K}^2 \preceq \sum_{e\in\mathcal{E}_h^i} h_e^{1-2|\gamma|} \|[\![\boldsymbol{w}_h]\!]\|_{0,e}^2 + \sum_{e\in\mathcal{E}_h^\partial} h_e^{1-2|\gamma|} \|\boldsymbol{g} - \boldsymbol{w}_h\|_{0,e}^2.$$

Proof. Apply Theorem 2.2 in [32] to each component. □

To avoid nonessential technical difficulties, we make the following assumption:

Assumption H: The Dirichlet boundary data $\boldsymbol{u}_D$ is the trace of a continuous function in $\boldsymbol{V}_h^*$ and $\boldsymbol{f}$ a piecewise polynomial function.

If this assumption is not satisfied, high order terms associated to the approximation of $\boldsymbol{u}_D$ and $\boldsymbol{f}$ would appear. Finally, to prove the local efficiency of our error estimator, we consider the following bubble functions. Let $B_K := \Pi_{i=1}^{d+1}\lambda_i$ be the element-bubble function associated to $K \in \mathcal{T}_h$, where $\{\lambda_i\}_{i=1}^{d+1}$ are the barycentric coordinates of K, and $B_e := \Pi_{\substack{i=1\\i\neq j}}^{d+1}\lambda_i$ be the face-bubble function associated to $e \subset \partial K$, where $j \in \{1, \ldots, d+1\}$ is the index such that $\lambda_j = 0$ on e.

Lemma 3.3. *The following estimates hold for all $\boldsymbol{v} \in \mathbb{P}_k(K)^d$, $K \in \mathcal{T}_h$, $\boldsymbol{\mu} \in \mathbb{P}_k(e)^d$, and $e \in \mathcal{E}_h$:*

$$\|\boldsymbol{v}\|_{0,K}^2 \preceq (\boldsymbol{v}, B_K\boldsymbol{v})_K, \qquad \|B_K\boldsymbol{v}\|_{0,K} \preceq \|\boldsymbol{v}\|_{0,K}, \qquad |\!|\!|B_K\boldsymbol{v}|\!|\!|_{1,K} \preceq \theta_K^{-1}\|\boldsymbol{v}\|_{0,K},$$
$$\|\boldsymbol{\mu}\|_{0,e}^2 \preceq (\boldsymbol{\mu}, B_e\boldsymbol{\mu})_e, \qquad \|B_e\boldsymbol{\mu}\|_{0,\omega_e} \preceq \nu^{1/4}\theta_e^{1/2}\|\boldsymbol{\mu}\|_{0,e}, \qquad |\!|\!|B_e\boldsymbol{\mu}|\!|\!|_{1,\omega_e} \preceq \nu^{1/4}\theta_e^{-1/2}\|\boldsymbol{\mu}\|_{0,e}.$$

Proof. The proof is an extension of Lemma 3.3 in [44]. □

3.2. A posteriori error estimator

For each $K \in \mathcal{T}_h$, we propose the following local error estimator

$$\begin{aligned}\eta_K^2 := {} & \theta_K^2\|\boldsymbol{f} + \nabla\cdot(\nu\mathrm{L}_h) - \nabla\cdot(\boldsymbol{u}_h^*\otimes\boldsymbol{\beta}) - \nabla p_h\|_{0,K}^2 + \nu\|\mathrm{L}_h - \nabla\boldsymbol{u}_h^*\|_{0,K}^2 + \nu\|\nabla\cdot\boldsymbol{u}_h^*\|_{0,K}^2 \\ & + \frac{1}{2}\sum_{e\in\mathcal{E}_h^i\cap\partial K}\left(\nu^{-1/2}\theta_e\|[\![\nu\mathrm{L}_h - (\boldsymbol{u}_h^*\otimes\boldsymbol{\beta}) - p_h\mathrm{I}]\!]\|_{0,e}^2 + \nu h_e^{-1}\|[\![\boldsymbol{u}_h^*]\!]\|_{0,e}^2\right) + \sum_{e\in\mathcal{E}_h^\partial\cap\partial K}\nu h_e^{-1}\|\boldsymbol{g}_D - \boldsymbol{u}_h^*\|_{0,e}^2\end{aligned} \tag{3.1}$$

and its global version given by $\eta_h := \left(\sum_{K\in\mathcal{T}_h}\eta_K^2\right)^{1/2}$. Here we recall that θ_K and θ_e were defined in Lemma 3.1.

The first three terms are the residuals associated to the equilibrium equation, the constitutive equation and the incompressibility condition, respectively, while the jumps across the faces refer to the continuity of the trace of $\boldsymbol{u}$ and the normal trace of $\nu\mathrm{L} - (\boldsymbol{u}\otimes\boldsymbol{\beta}) - p\mathrm{I}$, if the solution of the continuous problem had enough regularity.

To prove our main result, we combine two techniques. One of them consists of adapting, to our setting, the procedure followed in [2] for the Brinkman problem. However, in contrast to Brinkman equations, in our case the L^2-error of the scalar variable cannot be obtained directly from the formulation. That is why we employ the weighted function technique used by [7] in the context of the convection-diffusion equations. We emphasize that we keep track the dependence on ν and $\boldsymbol{\beta}$.

We start by introducing three lemmas that will allow us to prove the reliability of the error estimator.

Lemma 3.4. *Let* $(\mathrm{L}, \boldsymbol{u}, p)$ *and* $(\mathrm{L}_h, \boldsymbol{u}_h, p_h \widehat{\boldsymbol{u}}_h)$ *the solutions of* (1.1) *and* (2.2)*, respectively, and* $\boldsymbol{u}_h^*$ *the postprocessed velocity defined by* (2.5)*. Then*

$$\nu^{-1/2}\|p-p_h\|_{0,\mathcal{T}_h} \preceq \max\{1, C_{\nu,\boldsymbol{\beta}}\}\Bigg[\nu^{1/2}\|\mathrm{L}-\mathrm{L}_h\|_{0,\mathcal{T}_h} + \frac{\|\boldsymbol{\beta}\|_{\infty,\Omega}^{1/2}}{\mathsf{diam}(\Omega)^{1/2}}\|\boldsymbol{u}-\boldsymbol{u}_h^*\|_{0,\mathcal{T}_h}$$
$$+\sum_{K\in\mathcal{T}_h}\Bigg(\theta_K\|\boldsymbol{f}+\nabla\cdot(\nu\mathrm{L}_h)-\nabla\cdot(\boldsymbol{u}_h^*\otimes\boldsymbol{\beta})-\nabla p_h\|_{0,K} + \frac{1}{2}\sum_{e\in\mathcal{E}_h^i\cap\partial K}\nu^{-1/4}\theta_e^{1/2}\|[\![\nu\mathrm{L}_h-(\boldsymbol{u}_h^*\otimes\boldsymbol{\beta})-p_h\mathrm{I}]\!]\|_{0,e}\Bigg)$$
$$+\frac{\|\boldsymbol{\beta}\|_{\boldsymbol{W}^{1,\infty}(\Omega)}}{\nu^{1/2}}\sum_{K\in\mathcal{T}_h} h_K\|\boldsymbol{u}_h-\boldsymbol{u}_h^*\|_{0,K}\Bigg],$$

where $C_{\nu,\boldsymbol{\beta}} := \dfrac{\|\boldsymbol{\beta}\|_{\infty,\Omega}^{1/2}\mathsf{diam}(\Omega)^{1/2}}{\nu^{1/2}}$.

Proof. For $q \in L_0^2(\Omega)$ we know that ([30], Chapter 1, Corollary 2.4)

$$\nu^{-1/2}\|q\|_{0,\mathcal{T}_h} \preceq \sup_{\boldsymbol{w}\in H_0^1(\Omega)^d\setminus\{\boldsymbol{0}\}} \frac{(q,\nabla\cdot\boldsymbol{w})_{\mathcal{T}_h}}{\nu^{1/2}\|\nabla\boldsymbol{w}\|_{0,\mathcal{T}_h}}.$$

Since $p-p_h \in L_0^2(\Omega)$ (cf. (1.1e) and (2.2f)) we can use the above inf-sup condition, with $q = p-p_h$, to get an estimate for $\nu^{-1/2}\|p-p_h\|_{0,\mathcal{T}_h}$. In fact, let $\boldsymbol{w} \in H_0^1(\Omega)^d$. Then, integrating by parts, considering (1.1b), reordering terms and integrating by parts again , we obtain

$$\begin{aligned}(p-p_h,\nabla\cdot\boldsymbol{w})_{\mathcal{T}_h} &= -\nu(\nabla\cdot(\mathrm{L}-\mathrm{L}_h),\boldsymbol{w})_{\mathcal{T}_h} + (\nabla\cdot((\boldsymbol{u}-\boldsymbol{u}_h^*)\otimes\boldsymbol{\beta}),\boldsymbol{w})_{\mathcal{T}_h}\\ &\quad -(\boldsymbol{f}+\nabla\cdot(\nu\mathrm{L}_h)-\nabla\cdot(\boldsymbol{u}_h^*\otimes\boldsymbol{\beta})-\nabla p_h,\boldsymbol{w})_{\mathcal{T}_h} + \langle(p-p_h)\boldsymbol{n},\boldsymbol{w}\rangle_{\partial\mathcal{T}_h}\\ &= \nu(\mathrm{L}-\mathrm{L}_h,\nabla\boldsymbol{w})_{\mathcal{T}_h} - ((\boldsymbol{u}-\boldsymbol{u}_h^*)\otimes\boldsymbol{\beta},\nabla\boldsymbol{w})_{\mathcal{T}_h}\\ &\quad -(\boldsymbol{f}+\nabla\cdot(\nu\mathrm{L}_h)-\nabla\cdot(\boldsymbol{u}_h^*\otimes\boldsymbol{\beta})-\nabla p_h,\boldsymbol{w})_{\mathcal{T}_h}\\ &\quad +\langle[\![\nu\mathrm{L}_h-\boldsymbol{u}_h^*\otimes\boldsymbol{\beta}-p_h\mathrm{I}]\!],\boldsymbol{w}\rangle_{\mathcal{E}_h^i}. \end{aligned}\tag{3.2}$$

On the other hand, integrating by parts in (2.2b) and considering (2.2e), we have

$$(\boldsymbol{f}+\nabla\cdot(\nu\mathrm{L}_h)-\nabla\cdot(\boldsymbol{u}_h\otimes\boldsymbol{\beta})-\nabla p_h\,\boldsymbol{v})_{\mathcal{T}_h} = \langle\nu\mathrm{L}_h\boldsymbol{n}-(\boldsymbol{u}_h\otimes\boldsymbol{\beta})\boldsymbol{n}-p_h\boldsymbol{n},\boldsymbol{v}\rangle_{\partial\mathcal{T}_h\setminus\Gamma}\quad \forall\boldsymbol{v}\in\boldsymbol{V}_h^{1,c},\tag{3.3}$$

where $\boldsymbol{V}_h^{1,c} := \{\boldsymbol{v}\in H_0^1(\Omega)^d : \boldsymbol{v}|_K\in\mathbb{P}_1(K)^d\ \ \forall K\in\mathcal{T}_h\}$. Moreover, for $\boldsymbol{v}\in\boldsymbol{V}_h^{1,c}$ and $K\in\mathcal{T}_h$, we have that

$$\begin{aligned}-(\nabla\cdot(\boldsymbol{u}_h\otimes\boldsymbol{\beta}),\boldsymbol{v})_K &= (\boldsymbol{u}_h\otimes\boldsymbol{\beta},\nabla\boldsymbol{v})_K - \langle(\boldsymbol{u}_h\otimes\boldsymbol{\beta})\boldsymbol{n},\boldsymbol{v}\rangle_{\partial K\setminus\Gamma}\\ &= (\boldsymbol{u}_h\otimes\mathsf{P}_0\boldsymbol{\beta},\nabla\boldsymbol{v})_K + (\boldsymbol{u}_h\otimes(\mathsf{I}-\mathsf{P}_0)\boldsymbol{\beta},\nabla\boldsymbol{v})_K - \langle(\boldsymbol{u}_h\otimes\boldsymbol{\beta})\boldsymbol{n},\boldsymbol{v}\rangle_{\partial K\setminus\Gamma}\\ &= (\boldsymbol{u}_h^*\otimes\mathsf{P}_0\boldsymbol{\beta},\nabla\boldsymbol{v})_K + (\boldsymbol{u}_h\otimes(\mathsf{I}-\mathsf{P}_0)\boldsymbol{\beta},\nabla\boldsymbol{v})_K - \langle(\boldsymbol{u}_h\otimes\boldsymbol{\beta})\boldsymbol{n},\boldsymbol{v}\rangle_{\partial K\setminus\Gamma}\\ &= (\boldsymbol{u}_h^*\otimes\boldsymbol{\beta},\nabla\boldsymbol{v})_K + ((\boldsymbol{u}_h-\boldsymbol{u}_h^*)\otimes(\mathsf{I}-\mathsf{P}_0)\boldsymbol{\beta},\nabla\boldsymbol{v})_K - \langle(\boldsymbol{u}_h\otimes\boldsymbol{\beta})\boldsymbol{n},\boldsymbol{v}\rangle_{\partial K\setminus\Gamma}\\ &= -(\nabla\cdot(\boldsymbol{u}_h^*\otimes\boldsymbol{\beta}),\boldsymbol{v})_K + ((\boldsymbol{u}_h-\boldsymbol{u}_h^*)\otimes(\mathsf{I}-\mathsf{P}_0)\boldsymbol{\beta},\nabla\boldsymbol{v})_K\\ &\quad -\langle(\boldsymbol{u}_h\otimes\boldsymbol{\beta})\boldsymbol{n},\boldsymbol{v}\rangle_{\partial K\setminus\Gamma} + \langle(\boldsymbol{u}_h^*\otimes\boldsymbol{\beta})\boldsymbol{n},\boldsymbol{v}\rangle_{\partial K\setminus\Gamma},\end{aligned}$$

that combined with (3.3) result in

$$\begin{aligned}&(\boldsymbol{f}+\nabla\cdot(\nu\mathrm{L}_h)-\nabla\cdot(\boldsymbol{u}_h^*\otimes\boldsymbol{\beta})-\nabla p_h\,\boldsymbol{v})_{\mathcal{T}_h}\\ &\qquad= \langle[\![\nu\mathrm{L}_h-\boldsymbol{u}_h^*\otimes\boldsymbol{\beta}-p_h\mathrm{I}]\!],\boldsymbol{v}\rangle_{\mathcal{E}_h^i} - ((\boldsymbol{u}_h-\boldsymbol{u}_h^*)\otimes(\mathsf{I}-\mathsf{P}_0)\boldsymbol{\beta},\nabla\boldsymbol{v})_{\mathcal{T}_h}\quad\forall\boldsymbol{v}\in\boldsymbol{V}_h^{1,c},\end{aligned}\tag{3.4}$$

Then, combining (3.2) and (3.4) with $\boldsymbol{v} = \mathcal{C}_h\boldsymbol{w}$, we obtain

$$\begin{aligned}(p-p_h,\nabla\cdot\boldsymbol{w})_{\mathcal{T}_h} &= \nu(\mathrm{L}-\mathrm{L}_h,\nabla\boldsymbol{w})_{\mathcal{T}_h} - ((\boldsymbol{u}-\boldsymbol{u}_h^*)\otimes\boldsymbol{\beta},\nabla\boldsymbol{w})_{\mathcal{T}_h}\\ &\quad -(\boldsymbol{f}+\nabla\cdot(\nu\mathrm{L}_h)-\nabla\cdot(\boldsymbol{u}_h^*\otimes\boldsymbol{\beta})-\nabla p_h,(\mathcal{I}-\mathcal{C}_h)\boldsymbol{w})_{\mathcal{T}_h}\\ &\quad +\langle[\![\nu\mathrm{L}_h-\boldsymbol{u}_h^*\otimes\boldsymbol{\beta}-p_h\mathrm{I}]\!],(\mathcal{I}-\mathcal{C}_h)\boldsymbol{w}\rangle_{\mathcal{E}_h^i} + ((\boldsymbol{u}_h-\boldsymbol{u}_h^*)\otimes(\mathsf{I}-\mathsf{P}_0)\boldsymbol{\beta},\nabla\mathcal{C}_h\boldsymbol{w})_{\mathcal{T}_h}.\end{aligned}$$

The properties of the Clément interpolant in Lemma 3.1 and the regularity of the mesh imply

$$
\begin{aligned}
&(p-p_h,\nabla\cdot\boldsymbol{w})_{\mathcal{T}_h}\\
&\le \sum_{K\in\mathcal{T}_h}\nu\|\mathrm{L}-\mathrm{L}_h\|_{0,K}\|\nabla\boldsymbol{w}\|_{0,K}+\sum_{K\in\mathcal{T}_h}\|(\boldsymbol{u}-\boldsymbol{u}_h^*)\otimes\boldsymbol{\beta}\|_{0,K}\|\nabla\boldsymbol{w}\|_{0,K}\\
&\quad+\sum_{K\in\mathcal{T}_h}\|\boldsymbol{f}+\nabla\cdot(\nu\mathrm{L}_h)-\nabla\cdot(\boldsymbol{u}_h^*\otimes\boldsymbol{\beta})-\nabla p_h\|_{0,K}\|(\mathcal{I}-\mathcal{C}_h)\boldsymbol{w}\|_{0,K}\\
&\quad+\sum_{e\in\mathcal{E}_h^i}\|[\![\nu\mathrm{L}_h-(\boldsymbol{u}_h^*\otimes\boldsymbol{\beta})-p_h\mathrm{I}]\!]\|_{0,e}\|(\mathcal{I}-\mathcal{C}_h)\boldsymbol{w}\|_{0,e}+\sum_{K\in\mathcal{T}_h}\|\boldsymbol{u}_h-\boldsymbol{u}_h^*\|_{0,K}\|(\mathsf{I}-\mathsf{P}_0)\boldsymbol{\beta}\|_{\infty,K}\|\nabla\mathcal{C}_h\boldsymbol{w}\|_{0,K}\\
&\le\left(\nu^{1/2}\|\mathrm{L}-\mathrm{L}_h\|_{0,\mathcal{T}_h}+C_{\nu,\boldsymbol{\beta}}\frac{\|\boldsymbol{\beta}\|_{\infty,\Omega}^{1/2}}{\mathsf{diam}(\Omega)^{1/2}}\|\boldsymbol{u}-\boldsymbol{u}_h^*\|_{0,\mathcal{T}_h}\right)\nu^{1/2}\|\nabla\boldsymbol{w}\|_{0,\mathcal{T}_h}\\
&\quad+\left[\sum_{K\in\mathcal{T}_h}\left(\theta_K\|\boldsymbol{f}+\nabla\cdot(\nu\mathrm{L}_h)-\nabla\cdot(\boldsymbol{u}_h^*\otimes\boldsymbol{\beta})-\nabla p_h\|_{0,K}+\frac{1}{2}\sum_{e\in\mathcal{E}_h^i\cap\partial K}\nu^{-1/4}\theta_e^{1/2}\|[\![\nu\mathrm{L}_h-(\boldsymbol{u}_h^*\otimes\boldsymbol{\beta})-p_h\mathrm{I}]\!]\|_{0,e}\right)\right.\\
&\qquad\left.+C_0\frac{\|\boldsymbol{\beta}\|_{\boldsymbol{W}^{1,\infty}(\Omega)}}{\nu^{1/2}}\sum_{K\in\mathcal{T}_h}h_K\|\boldsymbol{u}_h-\boldsymbol{u}_h^*\|_{0,K}\right]|\!|\!|\boldsymbol{w}|\!|\!|_{1,\Omega}\\
&\le\max\{1,C_{\nu,\boldsymbol{\beta}}\}\left(\nu^{1/2}\|\mathrm{L}-\mathrm{L}_h\|_{0,\mathcal{T}_h}+\frac{\|\boldsymbol{\beta}\|_{\infty,\Omega}^{1/2}}{\mathsf{diam}(\Omega)^{1/2}}\|\boldsymbol{u}-\boldsymbol{u}_h^*\|_{0,\mathcal{T}_h}\right)\nu^{1/2}\|\nabla\boldsymbol{w}\|_{0,\mathcal{T}_h}\\
&\quad+\left[\sum_{K\in\mathcal{T}_h}\left(\theta_K\|\boldsymbol{f}+\nabla\cdot(\nu\mathrm{L}_h)-\nabla\cdot(\boldsymbol{u}_h^*\otimes\boldsymbol{\beta})-\nabla p_h\|_{0,K}+\frac{1}{2}\sum_{e\in\mathcal{E}_h^i\cap\partial K}\nu^{-1/4}\theta_e^{1/2}\|[\![\nu\mathrm{L}_h-(\boldsymbol{u}_h^*\otimes\boldsymbol{\beta})-p_h\mathrm{I}]\!]\|_{0,e}\right)\right.\\
&\qquad\left.+C_0\frac{\|\boldsymbol{\beta}\|_{\boldsymbol{W}^{1,\infty}(\Omega)}}{\nu^{1/2}}\sum_{K\in\mathcal{T}_h}h_K\|\boldsymbol{u}_h-\boldsymbol{u}_h^*\|_{0,K}\right]\max\{1,C_PC_{\nu,\boldsymbol{\beta}}\}\,\nu^{1/2}\|\nabla\boldsymbol{w}\|_{0,\mathcal{T}_h},
\end{aligned}
$$

where C_P is the Poincaré constant associated to Ω and C_0 joints the constants associated to P_0, the L^2-projection onto $\mathbb{P}_0(K)^d$. □

Now, to derive an estimate for the L^2-error of the velocity, we proceed as in [7] defining the auxiliary weighted function

$$\varphi := e^{-\psi}+\chi, \tag{3.5}$$

where χ is a positive constant to be determined below. Then, we have the following result.

Lemma 3.5. *Let* $(\mathrm{L},\boldsymbol{u},p)$ *and* $(\mathrm{L}_h,\boldsymbol{u}_h,p_h,\widehat{\boldsymbol{u}}_h)$*be the solutions of* (1.1) *and* (2.2)*, respectively, and* $\boldsymbol{u}_h^*$ *the postprocessed velocity defined by* (2.5)*. We set*

$$\chi := \frac{2\nu\ \mathsf{diam}(\Omega)\|\nabla\psi\|_{\infty,\Omega}^2\|e^{-\psi}\|_{\infty,\Omega}^2}{\|\boldsymbol{\beta}\|_{\infty,\Omega}\min\limits_{\boldsymbol{x}\in\Omega}e^{-\psi(\boldsymbol{x})}}+\frac{64\|\nabla\psi\|_{\infty,\Omega}^2}{\min\limits_{\boldsymbol{x}\in\Omega}e^{-\psi(\boldsymbol{x})}}C_P^2\left(\max\{1,C_{\nu,\boldsymbol{\beta}}\}\right)^2+\frac{3}{4}\min_{\boldsymbol{x}\in\Omega}e^{-\psi(\boldsymbol{x})}+1, \tag{3.6}$$

where $C_P>0$ *is the Poincaré inequality constant associated to* Ω*. Then*

$$
\begin{aligned}
\nu\|\mathrm{L}-\mathrm{L}_h\|_{0,\mathcal{T}_h}^2+\frac{\|\boldsymbol{\beta}\|_{\infty,\Omega}}{\mathsf{diam}(\Omega)}\|\boldsymbol{u}-\boldsymbol{u}_h^*\|_{0,\mathcal{T}_h}^2 &\preceq \max\{1,\|\varphi\|_{\infty,\Omega}^2\}\left(\max\{1,C_{\nu,\boldsymbol{\beta}}\}\right)^2\Bigg(\eta_h^2\\
&+\frac{\|\boldsymbol{\beta}\|_{\boldsymbol{W}^{1,\infty}(\Omega)}^2}{\nu}\sum_{K\in\mathcal{T}_h}h_K^2\|\boldsymbol{u}_h-\boldsymbol{u}_h^*\|_{0,K}^2+\max\left\{\frac{\nu}{\mathsf{diam}(\Omega)^2},\frac{\|\boldsymbol{\beta}\|_{\infty,\Omega}}{\mathsf{diam}(\Omega)},\frac{\|\boldsymbol{\beta}\|_{\infty,\Omega}^2}{\nu}\right\}\|\boldsymbol{u}_h-\widetilde{\boldsymbol{u}}_h\|_{0,\mathcal{T}_h}^2\Bigg),
\end{aligned}
$$

where $\widetilde{\boldsymbol{u}}_h^*$ *is the Oswald interpolant of* $\boldsymbol{u}_h^*$ *provided by Lemma 3.2.*

To prove this estimate, we need the following auxiliary result, adapted from Lemma 4.1 in [7].

Lemma 3.6. *Let* $e_{\mathrm{L}} := \mathrm{L} - \mathrm{L}_h$ *and* $e_{\boldsymbol{u}} := \boldsymbol{u} - \boldsymbol{u}_h^*$. *Then*

$$\left(\chi\nu - \frac{\nu^2 \mathsf{diam}(\Omega)\|\nabla\psi\|^2_{\infty,\Omega}\|e^{-\psi}\|^2_{\infty,\Omega}}{\|\boldsymbol{\beta}\|_{\infty,\Omega}\min_{\boldsymbol{x}\in\Omega} e^{-\psi(\boldsymbol{x})}}\right)\|e_{\mathrm{L}}\|^2_{0,\mathcal{T}_h} + \frac{1}{2}\min_{\boldsymbol{x}\in\Omega} e^{-\psi(\boldsymbol{x})}\frac{\|\boldsymbol{\beta}\|_{\infty,\Omega}}{\mathsf{diam}(\Omega)}\|e_{\boldsymbol{u}}\|^2_{0,\mathcal{T}_h}$$
$$\leq \nu(e_{\mathrm{L}}, \varphi e_{\mathrm{L}})_{\mathcal{T}_h} + \nu(e_{\mathrm{L}}\nabla\varphi, e_{\boldsymbol{u}})_{\mathcal{T}_h} - \frac{1}{2}((\boldsymbol{\beta}\cdot\nabla\varphi)e_{\boldsymbol{u}}, e_{\boldsymbol{u}})_{\mathcal{T}_h}.$$

Proof. From the definition of φ and the fact that $\boldsymbol{\beta}\cdot\nabla\psi \geq \frac{\|\boldsymbol{\beta}\|_{\infty,\Omega}}{\mathsf{diam}(\Omega)}$, we obtain

$$\nu(e_{\mathrm{L}}, \varphi e_{\mathrm{L}})_{\mathcal{T}_h} - \nu(e^{-\psi}e_{\mathrm{L}}\nabla\psi, e_{\boldsymbol{u}})_{\mathcal{T}_h} + \frac{1}{2}((\boldsymbol{\beta}\cdot\nabla\psi)e^{-\psi}e_{\boldsymbol{u}}, e_{\boldsymbol{u}})_{\mathcal{T}_h}$$
$$\geq \chi\nu\|e_{\mathrm{L}}\|^2_{0,\mathcal{T}_h} - \nu(e^{-\psi}e_{\mathrm{L}}\nabla\psi, e_{\boldsymbol{u}})_{\mathcal{T}_h} + \frac{\|\boldsymbol{\beta}\|_{\infty,\Omega}}{2\mathsf{diam}(\Omega)}(e^{-\psi}e_{\boldsymbol{u}}, e_{\boldsymbol{u}})_{\mathcal{T}_h}.$$

To bound the second term on the right hand side, we use Cauchy-Schwarz and Young's inequalities to obtain, for any $\delta > 0$, that

$$|(e^{-\psi}e_{\mathrm{L}}\nabla\psi, e_{\boldsymbol{u}})_{\mathcal{T}_h}| \leq \frac{1}{2}(\delta^{-1}\|\nabla\psi\|^2_{\infty,\Omega}\|e^{-\psi}\|_{\infty,\Omega}\|e_{\mathrm{L}}\|^2_{0,\mathcal{T}_h} + \delta\|e^{-\psi}\|_{\infty,\Omega}\|e_{\boldsymbol{u}}\|^2_{0,\mathcal{T}_h}).$$

Then, the results follows from taking $\delta = \dfrac{\|\boldsymbol{\beta}\|_{\infty,\Omega}\min_{\boldsymbol{x}\in\Omega} e^{-\psi(\boldsymbol{x})}}{2\nu\mathsf{diam}(\Omega)\|e^{-\psi}\|_{\infty,\Omega}}$, combining both inequalities and noticing that $\nabla\varphi = -\nabla\psi e^{-\psi}$. $\square$

Now, we proceed to prove Lemma 3.5.

Proof of Lemma 3.5. Let $\widetilde{\boldsymbol{u}}_h^* \in H^1(\Omega)^d$ the Oswald interpolation of $\boldsymbol{u}_h^*$, $e_{\mathrm{L}} = \mathrm{L} - \mathrm{L}_h$ and $e_{\boldsymbol{u}} = \boldsymbol{u} - \boldsymbol{u}_h^*$. Adding and subtracting $\varphi\nabla\widetilde{\boldsymbol{u}}_h^*$, and integrating by parts we obtain

$$\begin{aligned}\nu(e_{\mathrm{L}}, \varphi e_{\mathrm{L}})_{\mathcal{T}_h} &= \nu(\mathrm{L} - \mathrm{L}_h, \varphi\nabla(\boldsymbol{u} - \widetilde{\boldsymbol{u}}_h^*))_{\mathcal{T}_h} + \nu(\mathrm{L} - \mathrm{L}_h, \varphi(\nabla\widetilde{\boldsymbol{u}}_h^* - \mathrm{L}_h))_{\mathcal{T}_h}\\ &= -\nu((\mathrm{L} - \mathrm{L}_h)(\nabla\varphi), \boldsymbol{u} - \widetilde{\boldsymbol{u}}_h^*)_{\mathcal{T}_h} - \nu(\varphi\ \nabla\cdot(\mathrm{L} - \mathrm{L}_h), \boldsymbol{u} - \widetilde{\boldsymbol{u}}_h^*)_{\mathcal{T}_h}\\ &\quad + \nu\langle(\mathrm{L} - \mathrm{L}_h)\boldsymbol{n}, \varphi(\boldsymbol{u} - \widetilde{\boldsymbol{u}}_h^*)\rangle_{\partial\mathcal{T}_h} + \nu(\mathrm{L} - \mathrm{L}_h, \varphi(\nabla\widetilde{\boldsymbol{u}}_h^* - \mathrm{L}_h))_{\mathcal{T}_h}.\end{aligned}$$

Using equations (1.1), adding and subtracting terms and integrating by parts, we arrive at

$$\begin{aligned}\nu(e_{\mathrm{L}}, \varphi e_{\mathrm{L}})_{\mathcal{T}_h} &= -\nu(e_{\mathrm{L}}\nabla\varphi, e_{\boldsymbol{u}})_{\mathcal{T}_h} - \nu((\mathrm{L} - \mathrm{L}_h)(\nabla\varphi), \boldsymbol{u}_h^* - \widetilde{\boldsymbol{u}}_h^*)_{\mathcal{T}_h}\\ &\quad + (\boldsymbol{f} + \nabla\cdot(\nu\mathrm{L}_h) - \nabla\cdot(\boldsymbol{u}_h^*\otimes\boldsymbol{\beta}) - \nabla p_h, \varphi(\boldsymbol{u} - \widetilde{\boldsymbol{u}}_h^*))_{\mathcal{T}_h}\\ &\quad + \langle(\nu\mathrm{L} - (\boldsymbol{u}\otimes\boldsymbol{\beta}) - p\mathrm{I})\boldsymbol{n}, \varphi(\boldsymbol{u} - \widetilde{\boldsymbol{u}}_h^*)\rangle_{\partial\mathcal{T}_h\setminus\Gamma} - \langle(\nu\mathrm{L}_h - (\boldsymbol{u}_h^*\otimes\boldsymbol{\beta}) - p_h\mathrm{I})\boldsymbol{n}, \varphi(\boldsymbol{u} - \widetilde{\boldsymbol{u}}_h^*)\rangle_{\partial\mathcal{T}_h\setminus\Gamma}\\ &\quad + ((\boldsymbol{u} - \boldsymbol{u}_h^*)\otimes\boldsymbol{\beta}, \nabla(\varphi(\boldsymbol{u} - \widetilde{\boldsymbol{u}}_h^*)))_{\mathcal{T}_h} + ((p - p_h)\mathrm{I}, \nabla(\varphi(\boldsymbol{u} - \widetilde{\boldsymbol{u}}_h^*)))_{\mathcal{T}_h}\\ &\quad + \nu(\mathrm{L} - \mathrm{L}_h, \varphi(\nabla\widetilde{\boldsymbol{u}}_h^* - \mathrm{L}_h))_{\mathcal{T}_h}.\end{aligned}$$

Since $\boldsymbol{u} - \widetilde{\boldsymbol{u}}_h^* \in H_0^1(\Omega)^d$ (Lemma 3.2 with $\boldsymbol{g} = \boldsymbol{u}_D$) and $\nu\mathrm{L} - (\boldsymbol{u}\otimes\boldsymbol{\beta}) - p\mathrm{I} \in H(\mathrm{div}, \Omega)^d$, we have that

$$\begin{aligned}\nu(e_{\mathrm{L}}, \varphi e_{\mathrm{L}})_{\mathcal{T}_h} &= -\nu(e_{\mathrm{L}}\nabla\varphi, e_{\boldsymbol{u}})_{\mathcal{T}_h} - \nu((\mathrm{L} - \mathrm{L}_h)(\nabla\varphi), \boldsymbol{u}_h^* - \widetilde{\boldsymbol{u}}_h^*)_{\mathcal{T}_h} + \nu(\mathrm{L} - \mathrm{L}_h, \varphi(\nabla\widetilde{\boldsymbol{u}}_h^* - \mathrm{L}_h))_{\mathcal{T}_h}\\ &\quad + (\boldsymbol{f} + \nabla\cdot(\nu\mathrm{L}_h) - \nabla\cdot(\boldsymbol{u}_h^*\otimes\boldsymbol{\beta}) - \nabla p_h, \varphi(\boldsymbol{u} - \widetilde{\boldsymbol{u}}_h^*))_{\mathcal{T}_h}\\ &\quad - \langle(\nu\mathrm{L}_h - (\boldsymbol{u}_h^*\otimes\boldsymbol{\beta}) - p_h\mathrm{I})\boldsymbol{n}, \varphi(\boldsymbol{u} - \widetilde{\boldsymbol{u}}_h^*)\rangle_{\partial\mathcal{T}_h\setminus\Gamma}\\ &\quad + ((\boldsymbol{u} - \boldsymbol{u}_h^*)\otimes\boldsymbol{\beta}, \nabla(\varphi(\boldsymbol{u} - \widetilde{\boldsymbol{u}}_h^*)))_{\mathcal{T}_h} + (p - p_h, \nabla\cdot(\varphi(\boldsymbol{u} - \widetilde{\boldsymbol{u}}_h^*)))_{\mathcal{T}_h}.\end{aligned}$$

Then, from Lemma 3.6 and (3.4), we obtain that

$$\left(\chi\nu - \frac{\nu^2 \mathsf{diam}(\Omega)\|\nabla\psi\|^2_{\infty,\Omega}\|e^{-\psi}\|^2_{\infty,\Omega}}{\|\boldsymbol{\beta}\|_{\infty,\Omega}\min_{\boldsymbol{x}\in\Omega} e^{-\psi(\boldsymbol{x})}}\right)\|e_{\mathrm{L}}\|^2_{0,\mathcal{T}_h} + \frac{1}{2}\min_{\boldsymbol{x}\in\Omega} e^{-\psi(\boldsymbol{x})}\frac{\|\boldsymbol{\beta}\|_{\infty,\Omega}}{\mathsf{diam}(\Omega)}\|e_{\boldsymbol{u}}\|^2_{0,\mathcal{T}_h} \leq T_1 + T_2 + T_3, \quad (3.7)$$

where

$$
\begin{aligned}
T_1 := & -\nu((\mathrm{L}-\mathrm{L}_h)(\nabla\varphi), \boldsymbol{u}_h^* - \widetilde{\boldsymbol{u}}_h^*)_{\mathcal{T}_h} + \nu(\mathrm{L}-\mathrm{L}_h, \varphi(\nabla\widetilde{\boldsymbol{u}}_h^* - \mathrm{L}_h))_{\mathcal{T}_h} \\
& + (\boldsymbol{f} + \nabla\cdot(\nu\mathrm{L}_h) - \nabla\cdot(\boldsymbol{u}_h^*\otimes\boldsymbol{\beta}) - \nabla p_h, (\mathcal{I}-\mathcal{C}_h)(\varphi(\boldsymbol{u}-\widetilde{\boldsymbol{u}}_h^*)))_{\mathcal{T}_h} \\
& - \langle(\nu\mathrm{L}_h - (\boldsymbol{u}_h^*\otimes\boldsymbol{\beta}) - p_h\mathrm{I})\boldsymbol{n}, (\mathcal{I}-\mathcal{C}_h)(\varphi(\boldsymbol{u}-\widetilde{\boldsymbol{u}}_h^*))\rangle_{\partial\mathcal{T}_h\setminus\Gamma} \\
& - ((\boldsymbol{u}_h - \boldsymbol{u}_h^*)\otimes(\mathsf{I}-\mathsf{P}_0)\boldsymbol{\beta}, \nabla\mathcal{C}_h(\varphi(\boldsymbol{u}-\widetilde{\boldsymbol{u}}_h^*)))_{\mathcal{T}_h} \\
T_2 := & ((\boldsymbol{u}-\boldsymbol{u}_h^*)\otimes\boldsymbol{\beta}, \nabla(\varphi(\boldsymbol{u}-\widetilde{\boldsymbol{u}}_h^*)))_{\mathcal{T}_h} - \frac{1}{2}((\boldsymbol{\beta}\cdot\nabla\varphi)e_{\boldsymbol{u}}, e_{\boldsymbol{u}})_{\mathcal{T}_h} \\
T_3 := & ((p-p_h)\mathrm{I}, \nabla(\varphi(\boldsymbol{u}-\widetilde{\boldsymbol{u}}_h^*)))_{\mathcal{T}_h}.
\end{aligned}
$$

First, we set $\mu = (1/32)\min_{\boldsymbol{x}\in\Omega} e^{-\psi(\boldsymbol{x})}$. Thanks to Cauchy-Schwarz and Young's inequalities, the stability and approximation properties of the Clément interpolant, the approximation property of P_0 and the regularity of the family of meshes, we get that

$$
\begin{aligned}
T_1 \le & \frac{1}{4}\nu\|e_{\mathrm{L}}\|_{0,\mathcal{T}_h}^2 + \|\nabla\varphi\|_{\infty,\Omega}^2\nu\|\boldsymbol{u}_h^* - \widetilde{\boldsymbol{u}}_h^*\|_{0,\mathcal{T}_h}^2 + \frac{1}{4}\nu\|e_{\mathrm{L}}\|_{0,\mathcal{T}_h}^2 + 2\|\varphi\|_{\infty,\Omega}^2\nu\|\mathrm{L}_h - \nabla\boldsymbol{u}_h^*\|_{0,\mathcal{T}_h}^2 \\
& + 2\|\varphi\|_{\infty,\Omega}^2\nu\|\nabla(\boldsymbol{u}_h^* - \widetilde{\boldsymbol{u}}_h^*)\|_{0,\mathcal{T}_h}^2 + 6\mu|\!|\!|e_{\boldsymbol{u}}|\!|\!|_{1,\mathcal{T}_h}^2 + 6\mu|\!|\!|\boldsymbol{u}_h^* - \widetilde{\boldsymbol{u}}_h^*|\!|\!|_{1,\mathcal{T}_h}^2 \\
& + \frac{1}{4\mu}\|\varphi\|_{\infty,\Omega}^2\sum_{K\in\mathcal{T}_h}\theta_K^2\|\boldsymbol{f} + \nabla\cdot(\nu\mathrm{L}_h) - \nabla\cdot(\boldsymbol{u}_h^*\otimes\boldsymbol{\beta}) - \nabla p_h\|_{0,K}^2 \\
& + \frac{1}{4\mu}\|\varphi\|_{\infty,\Omega}^2\sum_{K\in\mathcal{T}_h}\frac{1}{2}\sum_{e\in\mathcal{E}_h^i\cap\partial K}\nu^{-1/2}\theta_e\|[\![\nu\mathrm{L}_h - (\boldsymbol{u}_h^*\otimes\boldsymbol{\beta}) - p_h\mathrm{I}]\!]\|_{0,e}^2 \\
& + \frac{1}{4\mu}C_0\frac{\|\boldsymbol{\beta}\|_{\boldsymbol{W}^{1,\infty}(\Omega)}^2}{\nu}\sum_{K\in\mathcal{T}_h}h_K^2\|\boldsymbol{u}_h - \boldsymbol{u}_h^*\|_{0,K}^2.
\end{aligned}
\tag{3.8}
$$

On the other hand, for $\boldsymbol{w}\in H_0^1(\Omega)^d$, we have

$$
\begin{aligned}
\frac{1}{2}(\nabla\cdot\boldsymbol{\beta}, \varphi|\boldsymbol{w}|^2)_{\mathcal{T}_h} &= -\frac{1}{2}(\boldsymbol{\beta}, \nabla(\varphi|\boldsymbol{w}|^2))_{\mathcal{T}_h} = -\frac{1}{2}(\boldsymbol{\beta}, \varphi\nabla|\boldsymbol{w}|^2)_{\mathcal{T}_h} - \frac{1}{2}(\boldsymbol{\beta}, |\boldsymbol{w}|^2\nabla\varphi)_{\mathcal{T}_h} \\
&= -(\boldsymbol{\beta}, \varphi(\nabla\boldsymbol{w})^t\boldsymbol{w})_{\mathcal{T}_h} - \frac{1}{2}(\boldsymbol{\beta}\cdot\nabla\varphi, |\boldsymbol{w}|^2)_{\mathcal{T}_h} = -((\boldsymbol{\beta}\cdot\nabla)\boldsymbol{w}, \varphi\boldsymbol{w})_{\mathcal{T}_h} - \frac{1}{2}((\boldsymbol{\beta}\cdot\nabla\varphi)\boldsymbol{w}, \boldsymbol{w})_{\mathcal{T}_h}
\end{aligned}
$$

and since $\nabla\cdot\boldsymbol{\beta} = 0$, we obtain that $((\boldsymbol{\beta}\cdot\nabla)\boldsymbol{w}, \varphi\boldsymbol{w})_{\mathcal{T}_h} = -\frac{1}{2}((\boldsymbol{\beta}\cdot\nabla\varphi)\boldsymbol{w}, \boldsymbol{w})_{\mathcal{T}_h}$.

Then, using again the fact that $\boldsymbol{u} - \widetilde{\boldsymbol{u}}_h \in H_0^1(\Omega)^d$, we can write

$$
\begin{aligned}
((\boldsymbol{u}-\boldsymbol{u}_h^*)\otimes\boldsymbol{\beta}, \nabla(\varphi(\boldsymbol{u}-\widetilde{\boldsymbol{u}}_h^*)))_{\mathcal{T}_h} &= -(\nabla\cdot((\boldsymbol{u}-\widetilde{\boldsymbol{u}}_h^*)\otimes\boldsymbol{\beta}), \varphi(\boldsymbol{u}-\widetilde{\boldsymbol{u}}_h^*))_{\mathcal{T}_h} + ((\widetilde{\boldsymbol{u}}_h^* - \boldsymbol{u}_h^*)\otimes\boldsymbol{\beta}, \nabla(\varphi(\boldsymbol{u}-\widetilde{\boldsymbol{u}}_h^*)))_{\mathcal{T}_h} \\
&= -((\boldsymbol{\beta}\cdot\nabla)(\boldsymbol{u}-\widetilde{\boldsymbol{u}}_h^*), \varphi(\boldsymbol{u}-\widetilde{\boldsymbol{u}}_h^*))_{\mathcal{T}_h} + ((\widetilde{\boldsymbol{u}}_h^* - \boldsymbol{u}_h^*)\otimes\boldsymbol{\beta}, \nabla(\varphi(\boldsymbol{u}-\widetilde{\boldsymbol{u}}_h^*)))_{\mathcal{T}_h} \\
&= \frac{1}{2}((\boldsymbol{\beta}\cdot\nabla\varphi)(\boldsymbol{u}-\widetilde{\boldsymbol{u}}_h^*), \boldsymbol{u}-\widetilde{\boldsymbol{u}}_h^*)_{\mathcal{T}_h} + ((\widetilde{\boldsymbol{u}}_h^* - \boldsymbol{u}_h^*)\otimes\boldsymbol{\beta}, (\boldsymbol{u}-\widetilde{\boldsymbol{u}}_h^*)\otimes\nabla\varphi)_{\mathcal{T}_h} \\
&\quad + ((\widetilde{\boldsymbol{u}}_h^* - \boldsymbol{u}_h^*)\otimes\boldsymbol{\beta}, \varphi\nabla(\boldsymbol{u}-\widetilde{\boldsymbol{u}}_h^*))_{\mathcal{T}_h},
\end{aligned}
$$

and then

$$
\begin{aligned}
T_2 &= -(\nabla e_{\boldsymbol{u}}, \varphi(\boldsymbol{u}_h^* - \widetilde{\boldsymbol{u}}_h^*)\otimes\boldsymbol{\beta})_{\mathcal{T}_h} - (\nabla(\boldsymbol{u}_h^* - \widetilde{\boldsymbol{u}}_h^*), \varphi(\boldsymbol{u}_h^* - \widetilde{\boldsymbol{u}}_h^*)\otimes\boldsymbol{\beta})_{\mathcal{T}_h} - \frac{1}{2}((\boldsymbol{\beta}\cdot\nabla\varphi)(\boldsymbol{u}_h^* - \widetilde{\boldsymbol{u}}_h^*), \boldsymbol{u}_h^* - \widetilde{\boldsymbol{u}}_h^*)_{\mathcal{T}_h} \\
&\le \frac{1}{8}\nu\|\nabla e_{\boldsymbol{u}}\|_{0,\mathcal{T}_h}^2 + 2\frac{\|\boldsymbol{\beta}\|_{\infty,\Omega}^2}{\nu}\|\varphi\|_{\infty,\Omega}^2\|\boldsymbol{u}_h^* - \widetilde{\boldsymbol{u}}_h^*\|_{0,\mathcal{T}_h}^2 + \frac{1}{2}\nu\|\nabla(\boldsymbol{u}_h^* - \widetilde{\boldsymbol{u}}_h^*)\|_{0,\mathcal{T}_h}^2 + \frac{1}{2}\frac{\|\boldsymbol{\beta}\|_{\infty,\Omega}^2}{\nu}\|\boldsymbol{u}_h^* - \widetilde{\boldsymbol{u}}_h^*\|_{0,\mathcal{T}_h}^2 \\
&\quad + \|\boldsymbol{\beta}\|_{\infty,\Omega}\|\nabla\varphi\|_{\infty,\Omega}\|\boldsymbol{u}_h^* - \widetilde{\boldsymbol{u}}_h^*\|_{0,\mathcal{T}_h}^2,
\end{aligned}
\tag{3.9}
$$

by using Cauchy-Schwarz and Young's inequalities.

Then, after integrating by part, we write

$$
\begin{aligned}
T_3 &= ((p-p_h)\nabla\varphi, \boldsymbol{u}-\widetilde{\boldsymbol{u}}_h^*)_{\mathcal{T}_h} + (p-p_h, \varphi\ \nabla\cdot(\boldsymbol{u}-\widetilde{\boldsymbol{u}}_h^*))_{\mathcal{T}_h} \\
&= ((p-p_h)\nabla\varphi, e_{\boldsymbol{u}})_{\mathcal{T}_h} + ((p-p_h)\nabla\varphi, \boldsymbol{u}_h^*-\widetilde{\boldsymbol{u}}_h^*)_{\mathcal{T}_h} - (p-p_h, \varphi\ \nabla\cdot\boldsymbol{u}_h^*)_{\mathcal{T}_h} + (p-p_h, \varphi\ \nabla\cdot(\boldsymbol{u}_h^*-\widetilde{\boldsymbol{u}}_h^*))_{\mathcal{T}_h} \\
&\le 2\mu\left(\max\{1, C_{\nu,\boldsymbol{\beta}}\}\right)^{-2}\nu^{-1}\|p-p_h\|_{0,\mathcal{T}_h}^2 \\
&\quad + \frac{1}{2\mu}\|\nabla\varphi\|_{\infty,\Omega}^2 C_P^2\left(\max\{1, C_{\nu,\boldsymbol{\beta}}\}\right)^2\nu\|\nabla e_{\boldsymbol{u}}\|_{0,\mathcal{T}_h}^2 + \frac{1}{2\mu}\|\nabla\varphi\|_{\infty,\Omega}^2\left(\max\{1, C_{\nu,\boldsymbol{\beta}}\}\right)^2\nu\|\boldsymbol{u}_h^*-\widetilde{\boldsymbol{u}}_h^*\|_{0,\mathcal{T}_h}^2 \\
&\quad + \frac{1}{2\mu}\|\varphi\|_{\infty,\Omega}^2\left(\max\{1, C_{\nu,\boldsymbol{\beta}}\}\right)^2\nu\|\nabla\cdot\boldsymbol{u}_h^*\|_{0,\mathcal{T}_h}^2 + \frac{1}{2\mu}d\|\varphi\|_{\infty,\Omega}^2\left(\max\{1, C_{\nu,\boldsymbol{\beta}}\}\right)^2\nu\|\nabla(\boldsymbol{u}_h^*-\widetilde{\boldsymbol{u}}_h^*)\|_{0,\mathcal{T}_h}^2.
\end{aligned}
\tag{3.10}
$$

Finally, after inserting (3.8), (3.9) and (3.10) in (3.7), Lemma 3.4, the definition of $\|\!|\cdot|\!\|_{\mathcal{T}_h}$, the facts that $\|\nabla e_{\boldsymbol{u}}\|_{0,\mathcal{T}_h} \preceq \|e_{\mathrm{L}}\|_{0,\mathcal{T}_h} + \|\mathrm{L}_h - \nabla\boldsymbol{u}_h^*\|_{0,\mathcal{T}_h}$ and $\nabla\varphi = -\nabla\psi e^{-\psi}$, we obtain

$$
\begin{aligned}
&\left(\chi\nu - \frac{\nu^2\mathsf{diam}(\Omega)\|\nabla\psi\|_{\infty,\Omega}^2\|e^{-\psi}\|_{\infty,\Omega}^2}{\|\boldsymbol{\beta}\|_{\infty,\Omega}\min_{\boldsymbol{x}\in\Omega}e^{-\psi(\boldsymbol{x})}} - \frac{32}{\min_{\boldsymbol{x}\in\Omega}e^{-\psi(\boldsymbol{x})}}\|\nabla\psi\|_{\infty,\Omega}^2 C_P^2\left(\max\{1, C_{\nu,\boldsymbol{\beta}}\}\right)^2\nu\right. \\
&\qquad\left. - \frac{3}{8}\nu\min_{\boldsymbol{x}\in\Omega}e^{-\psi(\boldsymbol{x})} - \frac{1}{2}\nu\right)\|e_{\mathrm{L}}\|_{0,\mathcal{T}_h}^2 + \frac{1}{4}\min_{\boldsymbol{x}\in\Omega}e^{-\psi(\boldsymbol{x})}\frac{\|\boldsymbol{\beta}\|_{\infty,\Omega}}{\mathsf{diam}(\Omega)}\|e_{\boldsymbol{u}}\|_{0,\mathcal{T}_h}^2 \\
&\quad \le C_{\psi,\Omega}\max\{1, \|\varphi\|_{\infty,\Omega}^2\}\left(\max\{1, C_{\nu,\boldsymbol{\beta}}\}\right)^2\left(\eta_h^2 + C_0\frac{\|\boldsymbol{\beta}\|_{\boldsymbol{W}^{1,\infty}(\Omega)}^2}{\nu}\sum_{K\in\mathcal{T}_h}h_K^2\|\boldsymbol{u}_h-\boldsymbol{u}_h^*\|_{0,K}^2\right. \\
&\qquad\qquad\left. + \max\left\{\frac{\nu}{\mathsf{diam}(\Omega)^2}, \frac{\|\boldsymbol{\beta}\|_{\infty,\Omega}}{\mathsf{diam}(\Omega)}, \frac{\|\boldsymbol{\beta}\|_{\infty,\Omega}^2}{\nu}\right\}\|\boldsymbol{u}_h^*-\widetilde{\boldsymbol{u}}_h^*\|_{0,\mathcal{T}_h}^2\right),
\end{aligned}
$$

where $C_{\psi,\Omega} > 0$ is a constant depending only on ψ and Ω.

Thus, by the choice of χ in (3.6), last expression becomes

$$
\begin{aligned}
&\frac{\chi\nu}{2}\|e_{\mathrm{L}}\|_{0,\mathcal{T}_h}^2 + \frac{1}{4}\min_{\boldsymbol{x}\in\Omega}e^{-\psi(\boldsymbol{x})}\frac{\|\boldsymbol{\beta}\|_{\infty,\Omega}}{\mathsf{diam}(\Omega)}\|e_{\boldsymbol{u}}\|_{0,\mathcal{T}_h}^2 \\
&\quad \le C_{\psi,\Omega}\max\{1, \|\varphi\|_{\infty,\Omega}^2\}\left(\max\{1, C_{\nu,\boldsymbol{\beta}}\}\right)^2\left(\eta_h^2 + C_0\frac{\|\boldsymbol{\beta}\|_{\boldsymbol{W}^{1,\infty}(\Omega)}}{\nu^{1/2}}\sum_{K\in\mathcal{T}_h}h_K\|\boldsymbol{u}_h-\boldsymbol{u}_h^*\|_{0,K}\right. \\
&\qquad\qquad\left. + \max\left\{\nu, \frac{\|\boldsymbol{\beta}\|_{\infty,\Omega}}{\mathsf{diam}(\Omega)}, \frac{\|\boldsymbol{\beta}\|_{\infty,\Omega}^2}{\nu}\right\}\|\boldsymbol{u}_h^*-\widetilde{\boldsymbol{u}}_h^*\|_{0,\mathcal{T}_h}^2\right).
\end{aligned}
$$

Thus, the result follows noticing that $\chi > 1$. □

The next lemmas provide us tools to prove local efficiency of the error estimator.

Lemma 3.7. *Let $e \in \mathcal{E}_h^i$, then*

$$
\begin{aligned}
\nu^{-1/2}\theta_e\|[\![\nu\mathrm{L}_h - (\boldsymbol{u}_h^*\otimes\boldsymbol{\beta}) - p_h\mathrm{I}]\!]\|_{0,e}^2 &\preceq \left(\max\{1, C_{\nu,\boldsymbol{\beta}}\}\right)^2\left(\nu\|\mathrm{L}-\mathrm{L}_h\|_{0,\omega_e}^2 + \frac{\|\boldsymbol{\beta}\|_{\infty,\Omega}}{\mathsf{diam}(\Omega)}\|\boldsymbol{u}-\boldsymbol{u}_h^*\|_{0,\omega_e}^2\right. \\
&\quad\left. + \nu^{-1}\|p-p_h\|_{0,\omega_e}^2\right) + \sum_{K\in\omega_e}\theta_K^2\|\boldsymbol{f} + \nabla\cdot(\nu\mathrm{L}_h) - \nabla\cdot(\boldsymbol{u}_h^*\otimes\boldsymbol{\beta}) - \nabla p_h\|_{0,K}^2.
\end{aligned}
$$

Proof. For any $\boldsymbol{v} \in H_0^1(\omega_e)^d$ we have

$$\langle [\![\nu \mathrm{L}_h - (\boldsymbol{u}_h^* \otimes \boldsymbol{\beta}) - p_h \mathrm{I}]\!], \boldsymbol{v}\rangle_e = \sum_{K\in\omega_e} (\langle \nu(\mathrm{L}_h - \mathrm{L})\boldsymbol{n}, \boldsymbol{v}\rangle_{\partial K} + \langle ((\boldsymbol{u}-\boldsymbol{u}_h^*)\otimes\boldsymbol{\beta})\boldsymbol{n}, \boldsymbol{v}\rangle_{\partial K} + \langle (p-p_h)\boldsymbol{n}, \boldsymbol{v}\rangle_{\partial K})$$

$$= \sum_{K\in\omega_e} ((\nu(\mathrm{L}_h-\mathrm{L}), \nabla \boldsymbol{v})_K + (\nu\nabla\cdot(\mathrm{L}_h-\mathrm{L}), \boldsymbol{v})_K + (((\boldsymbol{u}-\boldsymbol{u}_h^*)\otimes\boldsymbol{\beta}), \nabla\boldsymbol{v}\rangle_{\partial K} + (\nabla\cdot((\boldsymbol{u}-\boldsymbol{u}_h^*)\otimes\boldsymbol{\beta}), \boldsymbol{v}\rangle_{\partial K}$$

$$+ (\nabla(p-p_h), \boldsymbol{v})_K + (p-p_h, \nabla\cdot\boldsymbol{v})_K)$$

$$= \sum_{K\in\omega_e} ((\nu(\mathrm{L}_h-\mathrm{L}), \nabla\boldsymbol{v})_K + ((\boldsymbol{u}-\boldsymbol{u}_h^*)\otimes\boldsymbol{\beta}, \nabla\boldsymbol{v})_K + (p-p_h, \nabla\cdot\boldsymbol{v})_K$$

$$+ (\boldsymbol{f} + \nabla\cdot(\nu\mathrm{L}_h) - \nabla\cdot(\boldsymbol{u}_h^*\otimes\boldsymbol{\beta}) - \nabla p_h, \boldsymbol{v})_K)$$

$$\leq \sum_{K\in\omega_e}\Bigg(\nu^{1/2}\|\mathrm{L}-\mathrm{L}_h\|_{0,K} + \mathsf{diam}(\Omega)\frac{\|\boldsymbol{\beta}\|_{\infty,\Omega}^{1/2}}{\nu^{1/2}\mathsf{diam}(\Omega)^{1/2}}\frac{\|\boldsymbol{\beta}\|_{\infty,\Omega}^{1/2}}{\mathsf{diam}(\Omega)^{1/2}}\|\boldsymbol{u}-\boldsymbol{u}_h^*\|_{0,K} + \nu^{-1/2}\|p-p_h\|_{0,K}$$

$$+ \theta_K\|\boldsymbol{f}+\nabla\cdot(\nu\mathrm{L}_h) - \nabla\cdot(\boldsymbol{u}_h^*\otimes\boldsymbol{\beta}) - \nabla p_h\|_{0,K}\Bigg) T_{\boldsymbol{v}},$$

where $T_{\boldsymbol{v}} := 2\nu^{1/2}\|\nabla\boldsymbol{v}\|_{0,K} + \nu^{1/2}\|\nabla\cdot\boldsymbol{v}\|_{0,K} + \theta_K^{-1}\|\boldsymbol{v}\|_{0,K}$.

Then, taking $\boldsymbol{v} := B_e[\![\nu\mathrm{L}_h - (\boldsymbol{u}_h^*\otimes\boldsymbol{\beta}) - p_h\mathrm{I}]\!]$ and applying Lemma 3.3, we get

$$T_{\boldsymbol{v}} \preceq |\!|\!|\boldsymbol{v}|\!|\!|_{1,K} + \theta_e^{-1}\|\boldsymbol{v}\|_{0,K} \preceq \nu^{1/4}\theta_e^{-1/2}\|[\![\nu\mathrm{L}_h - (\boldsymbol{u}_h^*\otimes\boldsymbol{\beta}) - p_h\mathrm{I}]\!]\|_{0,e}.$$

The result follows from Lemma 3.3 and the shape-regularity assumption. □

Lemma 3.8. *For any element $K \in \mathcal{T}_h$ we have*

$$\theta_K\|\boldsymbol{f}+\nabla\cdot(\nu\mathrm{L}_h) - (\boldsymbol{u}_h^*\otimes\boldsymbol{\beta}) - \nabla p_h\|_{0,K}$$

$$\preceq \max\{1, C_{\nu,\boldsymbol{\beta}}\}\left(\nu^{1/2}\|\mathrm{L}-\mathrm{L}_h\|_{0,K} + \frac{\|\boldsymbol{\beta}\|_{\infty,\Omega}^{1/2}}{\mathsf{diam}(\Omega)^{1/2}}\|\boldsymbol{u}-\boldsymbol{u}_h^*\|_{0,K} + \nu^{-1/2}\|p-p_h\|_{0,K}\right).$$

Proof. Let $\boldsymbol{v} = \boldsymbol{f}+\nabla\cdot(\nu\mathrm{L}_h) - (\boldsymbol{u}_h^*\otimes\boldsymbol{\beta}) - \nabla p_h$ then

$$(\boldsymbol{v}, B_K\boldsymbol{v})_K = -\nu(\nabla\cdot(\mathrm{L}-\mathrm{L}_h), B_K\boldsymbol{v})_K + (\nabla\cdot((\boldsymbol{u}-\boldsymbol{u}_h^*)\otimes\boldsymbol{\beta}), B_K\boldsymbol{v})_K + (\nabla(p-p_h), B_K\boldsymbol{v})_K$$

$$= \nu(\mathrm{L}-\mathrm{L}_h, \nabla B_K\boldsymbol{v})_K - ((\boldsymbol{u}-\boldsymbol{u}_h^*)\otimes\boldsymbol{\beta}, \nabla B_K\boldsymbol{v})_K - (p-p_h, \nabla\cdot B_K\boldsymbol{v})_K$$

$$\preceq (\nu^{1/2}\|\mathrm{L}-\mathrm{L}_h\|_{0,K} + \mathsf{diam}(\Omega)C_{\nu,\boldsymbol{\beta}}\frac{\|\boldsymbol{\beta}\|_{\infty,\Omega}^{1/2}}{\mathsf{diam}(\Omega)^{1/2}}\|\boldsymbol{u}-\boldsymbol{u}_h^*\|_{0,K} + \nu^{-1/2}\|p-p_h\|_{0,K})|\!|\!|B_K\boldsymbol{v}|\!|\!|_{1,K}.$$

The result follows from Lemma 3.3. □

Now, to derive upper bounds for the jump of the velocity we will decompose $\nu h_e^{-1}\|[\![\boldsymbol{u}_h^*]\!]\|_{0,e}^2$ into $\nu h_e^{-1}\|\mathsf{P}_{\mathsf{M}_0}[\![\boldsymbol{u}_h^*]\!]\|_{0,e}^2$ and $\nu h_e^{-1}\|(\mathsf{Id}-\mathsf{P}_{\mathsf{M}_0})[\![\boldsymbol{u}_h^*]\!]\|_{0,e}^2$, where, $\mathsf{P}_{\mathsf{M}_0}$ is the L^2-orthogonal projection into

$$\mathsf{M}_{0,h} := \{\boldsymbol{\mu}\in L^2(\mathcal{E}_h)^d : \boldsymbol{\mu}|_e \in \mathbb{P}_0(e)^d \quad \forall e\in\mathcal{E}_h\}.$$

Then, Lemmas 3.4 and 3.5 in [19], adapted to vector-valued functions and considering the approximate velocity instead of its postprocessing, imply

$$h_e^{-1}\|\mathsf{P}_{\mathsf{M}_0}[\![\boldsymbol{u}_h^*]\!]\|_{0,e}^2 \preceq \|\mathrm{L}_h - \nabla\boldsymbol{u}_h^*\|_{0,\omega_e}^2 \quad \text{for } k\geq 1, \tag{3.11}$$

and

$$h_e^{-1}\|(\mathsf{Id}-\mathsf{P}_{\mathsf{M}_0})[\![\boldsymbol{u}_h^*]\!]\|_{0,e}^2 \preceq \|\nabla(\boldsymbol{u}-\boldsymbol{u}_h^*)\|_{0,\omega_e}^2, \tag{3.12}$$

for each face $e\in\mathcal{E}_h$.

3.3. The main results

We define, on each $K \in \mathcal{T}_h$, the local error

$$\mathsf{e}_K^2 := \nu\|\mathrm{L} - \mathrm{L}_h\|_{0,K}^2 + \frac{\|\boldsymbol{\beta}\|_{\infty,\Omega}}{\mathsf{diam}(\Omega)}\|\boldsymbol{u} - \boldsymbol{u}_h^*\|_{0,K}^2 + \nu\|\nabla(\boldsymbol{u} - \boldsymbol{u}_h^*)\|_{0,K}^2 + \nu^{-1}\|p - p_h\|_{0,K}^2, \tag{3.13}$$

and its global version given by $\mathsf{e}_h := \left(\sum_{K\in\mathcal{T}_h} \mathsf{e}_K^2\right)^{1/2}$.

Now, we state and prove reliability and local efficiency results of our *a posteriori* error estimator (3.1).

Theorem 3.1 (Reliability)**.** *Let* φ *as in* (3.5). *Then*

$$\mathsf{e}_h \preceq \max\{1, \|\varphi\|_{\infty,\Omega}\} \max\{1, C_{\nu,\boldsymbol{\beta}}\}\Bigg(\eta_h + \frac{\|\boldsymbol{\beta}\|_{\boldsymbol{W}^{1,\infty}(\Omega)}}{\nu^{1/2}} \sum_{K\in\mathcal{T}_h} h_K\|\boldsymbol{u}_h - \boldsymbol{u}_h^*\|_{0,K} + \max\left\{\frac{\nu}{\mathsf{diam}(\Omega)^2}, \frac{\|\boldsymbol{\beta}\|_{\infty,\Omega}}{\mathsf{diam}(\Omega)}, \frac{\|\boldsymbol{\beta}\|_{\infty,\Omega}^2}{\nu}\right\}^{1/2} \sum_{e\in\mathcal{E}_h} h_e^{1/2}\|[\![\boldsymbol{u}_h^*]\!]\|_{0,e}\Bigg).$$

Proof. Thanks to Lemmas 3.4, 3.5, the definition of $C_{\nu,\boldsymbol{\beta}}$ and the fact that, for each $K \in \mathcal{T}_h$, $\nu^{1/2}\|\nabla(\boldsymbol{u} - \boldsymbol{u}_h^*)\|_{0,K} \preceq \nu^{1/2}\|\mathrm{L} - \mathrm{L}_h\|_{0,K} + \eta_K$, we get

$$\begin{aligned}\nu\|\mathrm{L} - \mathrm{L}_h\|_{0,\mathcal{T}_h}^2 &+ \|\!|\boldsymbol{u} - \boldsymbol{u}_h|\!\|_{1,\mathcal{T}_h}^2 + \nu^{-1}\|p - p_h\|_{0,\mathcal{T}_h}^2 \\ &\preceq \max\{1, \|\varphi\|_{\infty,\Omega}^2\}\left(\max\{1, C_{\nu,\boldsymbol{\beta}}\}\right)^2 \Bigg(\eta_h^2 + \frac{\|\boldsymbol{\beta}\|_{\boldsymbol{W}^{1,\infty}(\Omega)}^2}{\nu} \sum_{K\in\mathcal{T}_h} h_K^2\|\boldsymbol{u}_h - \boldsymbol{u}_h^*\|_{0,K}^2 \\ &\qquad + \max\left\{\frac{\nu}{\mathsf{diam}(\Omega)^2}, \frac{\|\boldsymbol{\beta}\|_{\infty,\Omega}}{\mathsf{diam}(\Omega)}, \frac{\|\boldsymbol{\beta}\|_{\infty,\Omega}^2}{\nu}\right\} \|\boldsymbol{u}_h^* - \widetilde{\boldsymbol{u}}_h^*\|_{0,\mathcal{T}_h}^2\Bigg).\end{aligned}$$

The result follows from taking $\boldsymbol{w}_h = \boldsymbol{u}_h^*$ in Lemma 3.2 to bound the last term on the right-hand side. □

Remark 3.1. *In Theorem 3.1 we have tracked the dependence on* φ*, because depends on* χ*, on* ν *and* $\boldsymbol{\beta}$*. In fact, recalling* (3.5)*, we get that*

$$\|\varphi\|_{\infty,\Omega} \le C_{\psi,\Omega} \max\left\{1, \|\chi\|_{\infty,\Omega}\right\} \le C_{\psi,\Omega}\left(\max\{1, C_{\nu,\boldsymbol{\beta}}^{-1}, C_{\nu,\boldsymbol{\beta}}\}\right)^2.$$

Theorem 3.2 (Efficiency)**.** *Let* $K \in \mathcal{T}_h$*,* $\mathsf{e}_{\omega_K} := \left(\sum_{K'\in\omega_K} \mathsf{e}_{\omega_K}^2\right)^{1/2}$ *and* $\omega_K := \{K' \in \mathcal{T}_h : K' \in \omega_e \text{ and } e \in \mathcal{E}_h \cap \partial K\}$*, then for* $k \ge 1$*,*

$$\eta_K \preceq \max\{1, C_{\nu,\boldsymbol{\beta}}\}\,\mathsf{e}_{\omega_K}.$$

Proof. By definition of η_K, lemmas 3.7–3.8, equations (3.11)-(3.12) and inequalities $\|\mathrm{L}_h - \nabla\boldsymbol{u}_h^*\|_{0,K} \le \|\mathrm{L} - \mathrm{L}_h\|_{0,K} + \|\nabla(\boldsymbol{u} - \boldsymbol{u}_h^*)\|_{0,K}$ and $\|\nabla\cdot\boldsymbol{u}_h^*\|_{0,K} = \|\nabla\cdot(\boldsymbol{u} - \boldsymbol{u}_h^*)\|_{0,K} \preceq \|\nabla(\boldsymbol{u} - \boldsymbol{u}_h^*)\|_{0,K}$, we have that

$$\begin{aligned}\eta_K^2 &\preceq \left(\max\{1, C_{\nu,\boldsymbol{\beta}}\}\right)^2\left(\nu\|\mathrm{L} - \mathrm{L}_h\|_{0,K}^2 + \frac{\|\boldsymbol{\beta}\|_{\infty,\Omega}}{\mathsf{diam}(\Omega)}\|\boldsymbol{u} - \boldsymbol{u}_h^*\|_{0,K}^2 + \nu^{-1}\|p - p_h\|_{0,K}^2\right) + \nu\|\mathrm{L}_h - \nabla\boldsymbol{u}_h^*\|_{0,K}^2 \\ &\quad + \nu\|\nabla\cdot\boldsymbol{u}_h^*\|_{0,K}^2 + \left(\max\{1, C_{\nu,\boldsymbol{\beta}}\}\right)^2\left(\nu\|\mathrm{L} - \mathrm{L}_h\|_{0,\omega_K}^2 + \frac{\|\boldsymbol{\beta}\|_{\infty,\Omega}}{\mathsf{diam}(\Omega)}\|\boldsymbol{u} - \boldsymbol{u}_h^*\|_{0,\omega_K}^2 + \nu^{-1}\|p - p_h\|_{0,\omega_K}^2\right) \\ &\quad + \sum_{K'\in\omega_K} \theta_{K'}^2\|\boldsymbol{f} + \nabla\cdot(\nu\mathrm{L}_h) - (\boldsymbol{u}_h^* \otimes \boldsymbol{\beta}) - \nabla p_h\|_{0,K'}^2 + \nu\|\mathrm{L}_h - \nabla\boldsymbol{u}_h^*\|_{0,\omega_K}^2 + \nu\|\nabla(\boldsymbol{u} - \boldsymbol{u}_h^*)\|_{0,\omega_K}^2 \\ &\preceq \left(\max\{1, C_{\nu,\boldsymbol{\beta}}\}\right)^2\left(\nu\|\mathrm{L} - \mathrm{L}_h\|_{0,\omega_K}^2 + \|\!|\boldsymbol{u} - \boldsymbol{u}_h^*|\!\|_{1,\omega_K}^2 + \nu^{-1}\|p - p_h\|_{0,\omega_K}^2\right),\end{aligned}$$

and the result follows. □

4. Numerical experiments

In this section, we carry out numerical simulations, for $d = 3$, to verify our main results in Theorems 3.1 and 3.2. To satisfy condition we consider,as in [5], the stabilization parameter τ given by

$$\tau = \frac{1}{2\nu} \max_{\boldsymbol{x}\in\mathcal{T}_h} \boldsymbol{\beta}(\boldsymbol{x}) \cdot \boldsymbol{n} + 1.$$

The values of the polynomial degree and physical parameters $\boldsymbol{\beta}$ and ν will be specified on each example.

Let us define the errors $\mathsf{e}_{\mathrm{L}} := \nu^{1/2}\|\mathrm{L}-\mathrm{L}_h\|_{0,\mathcal{T}_h}$, $\mathsf{e}_{\boldsymbol{u}} := |\!|\!|\boldsymbol{u}-\boldsymbol{u}_h^*|\!|\!|_{1,\mathcal{T}_h}$, $\mathsf{e}_p := \nu^{-1/2}\|p-p_h\|_{0,\mathcal{T}_h}$, the estimator terms η_i $(i = 1, \ldots, 5)$

$$\eta_1^2 := \sum_{K\in\mathcal{T}_h} \theta_K^2 \|\boldsymbol{f} + \nabla\cdot(\nu\mathrm{L}_h) - \nabla\cdot(\boldsymbol{u}_h^*\otimes\boldsymbol{\beta}) - \nabla p_h\|_{0,K}^2, \quad \eta_2^2 := \nu\|\mathrm{L}_h - \nabla\boldsymbol{u}_h^*\|_{0,\mathcal{T}_h}^2,$$

$$\eta_3^2 := \nu\|\nabla\cdot\boldsymbol{u}_h^*\|_{0,\mathcal{T}_h}^2, \quad \eta_4^2 := \nu^{-1/2}\sum_{e\in\mathcal{E}_h} \theta_e \|[\![\nu\mathrm{L}_h - (\boldsymbol{u}_h^*\otimes\boldsymbol{\beta}) - p_h\mathrm{I}]\!]\|_{0,e}^2 \quad \text{and} \quad \eta_5^2 := \nu\sum_{e\in\mathcal{E}_h} h_e^{-1}\|[\![\boldsymbol{u}_h^*]\!]\|_{0,e}^2,$$

and the effectivity index $\mathsf{eff} := \eta_h/\mathsf{e}_h$. The experimental orders of convergence will be computed in terms of the number of elements N and we will use the fact that $h \simeq N^{-1/3}$. We also include, on each table, a column with the size of the linear system that we solve, N_{sist}, to quantify the computational effort in each case. The implementation of the HDG method was based on [23], an efficient vectorized implementation of the HDG method for linear variable coefficient reaction-diffusion problems in polyhedral domains.

For the tests that include adaptivity, we use the strategy:

(i) Start with a coarse mesh $\mathcal{T}_h$.

(ii) Solve the discrete problem on the current mesh $\mathcal{T}_h$.

(iii) Compute η_K for each $K \in \mathcal{T}_h$.

(iv) Mark each $K' \in \mathcal{T}_h$ such that $\eta_{K'} \geq \theta \max_{K\in\mathcal{T}_h} \eta_K$, with $\theta \in [0, 1]$ and refine it using `Tetgen` (see [43]).

(v) Consider this new mesh as $\mathcal{T}_h$ and, unless a prescribed stopping criteria is satisfied, go to (ii).

4.1. A smooth solution

For this test case, we choose $\nu = 1$, $\boldsymbol{\beta} = (x, y, -2z)$ and $\Omega =]0, 1[\times]0, 1[\times]0, 1[$. The source term $\boldsymbol{f}$ and the boundary data $\boldsymbol{u}_D$ are chosen such that the exact solution of the problem is given by $\boldsymbol{u} := (u_1, u_2, u_3)$, where $u_1(x_1, x_2, x_3) := 2x_1^2x_2x_3$, $u_2(x_1, x_2, x_3) := -x_1x_2^2x_3$, $u_3(x_1, x_2, x_3) := -x_1x_2x_3^2$, and $p(x_1, x_2.x_3) := x_1 - 1/2$.

k	N	N_{sist}	e_{L}	order	$\mathsf{e}_{\boldsymbol{u}}$	order	e_p	order
	6	168	5.79e-01	–	2.26e-01	–	1.27e-01	–
	48	1,128	1.71e-01	1.76	6.28e-02	1.84	2.76e-02	2.20
1	384	8,160	4.52e-02	1.92	1.62e-02	1.95	6.24e-03	2.15
	3,072	61,824	1.15e-02	1.97	4.11e-03	1.98	1.45e-03	2.11
	24,576	480,786	2.91e-03	1.99	1.03e-03	1.99	3.42e-04	2.09
	6	330	1.28e-01	–	5.36e-02	–	3.87e-02	–
	48	2,208	1.78e-02	2.85	6.99e-03	2.94	3.69e-03	3.39
2	384	15,936	2.32e-03	2.94	8.91e-04	2.97	3.96e-04	3.22
	3,072	120,576	2.96e-04	2.97	1.12e-04	2.99	4.59e-05	3.11
	24,576	936,960	3.74e-05	2.98	1.41e-05	2.99	5.43e-06	3.08
	6	546	9.77e-03	–	3.20e-03	–	5.94e-03	–
	48	3,648	7.80e-04	3.65	2.47e-04	3.69	2.52e-04	4.56
3	384	26,304	5.35e-05	3.87	1.69e-05	3.87	1.29e-05	4.29
	3,072	198,912	3.49e-06	3.94	1.10e-06	3.94	7.23e-07	4.15
	24,576	1,545,216	2.23e-07	3.97	7.05e-08	3.97	4.27e-08	4.08

Table 1: History of convergence of the error terms for the Example 4.1 ($\nu = 1$).

k	N	η_1	order	η_2	order	η_3	order	η_4	order	η_5	order	eff
1	6	3.76e-01	–	1.09e-01	–	3.94e-02	–	7.42e-01	–	1.38e-01	–	1.342
	48	1.09e-01	1.79	3.82e-02	1.52	1.45e-02	1.44	2.39e-01	1.64	4.17e-02	1.72	1.455
	384	2.84e-02	1.93	1.06e-02	1.85	3.96e-03	1.87	6.66e-02	1.84	1.11e-02	1.90	1.530
	3,072	7.24e-03	1.97	2.75e-03	1.95	1.02e-03	1.97	1.75e-02	1.93	2.86e-03	1.96	1.572
	24,576	1.82e-03	1.99	6.97e-04	1.98	2.60e-04	1.96	4.49e-03	1.97	7.22e-04	1.99	1.591
2	6	1.82e-01	–	3.55e-02	–	1.59e-02	–	1.74e-01	–	2.67e-02	–	1.775
	48	2.41e-02	2.91	5.03e-03	2.82	2.26e-03	2.81	2.84e-02	2.61	3.61e-03	2.89	1.948
	384	3.11e-03	2.96	6.61e-04	2.93	2.95e-04	2.94	3.92e-03	2.86	4.65e-04	2.96	2.019
	3,072	3.94e-04	2.98	8.45e-05	2.97	3.75e-05	2.98	5.12e-04	2.94	5.90e-05	2.98	2.052
	24,576	4.97e-05	2.99	1.07e-05	2.99	4.76e-06	2.98	6.56e-05	2.97	7.42e-06	2.99	2.068
3	6	3.56e-02	–	1.39e-03	–	4.60e-04	–	1.56e-02	–	6.32e-04	–	3.273
	48	2.27e-03	3.97	1.09e-04	3.68	3.86e-05	3.58	1.41e-03	3.47	5.40e-05	3.55	3.124
	384	1.45e-04	3.97	7.35e-06	3.89	2.60e-06	3.89	9.97e-05	3.82	3.68e-06	3.88	3.061
	3,072	9.19e-06	3.98	4.75e-07	3.95	1.67e-07	3.96	6.59e-06	3.92	2.38e-07	3.95	3.034
	24,576	5.79e-07	3.99	3.02e-08	3.98	1.07e-08	3.96	4.23e-07	3.96	1.51e-08	3.98	3.021

Table 2: History of convergence of the terms composing the error estimator for the Example 4.1 ($\nu = 1$).

Table 1 shows the history of convergence of the error of each variable when the number of elements N increases by a factor of 8. We see that all the error terms converge with optimal order of $k+1$, exactly as the error estimates in [5] predicted. In addition, we see in Table 2 that each term of the error estimator converge with order $k+1$. Moreover, the effectivity index remains bounded.

We repeat the experiment considering now $\nu = 10^{-1}$ and $\nu = 10^{-2}$. As Tables 3–6 show, similar conclusions can be drawn regarding the optimal order of convergence of the error and the estimator. The last column of Tables 4 and 6 displays the effectivity index. It remains bounded for each polynomial degree k.

k	N	N_{dof}	e_{L}	order	$\mathsf{e}_{\boldsymbol{u}}$	order	e_p	order
1	6	168	2.12e-01	–	8.99e-02	–	1.13e-01	–
	48	1,128	7.63e-02	1.47	2.86e-02	1.65	2.74e-02	2.05
	384	8,160	2.24e-02	1.77	7.96e-03	1.84	6.00e-03	2.19
	3,072	61,824	6.07e-03	1.88	2.14e-03	1.89	1.31e-03	2.20
	24,576	480,786	1.59e-03	1.94	5.60e-04	1.93	2.96e-04	2.14
2	6	330	6.40e-02	–	2.82e-02	–	4.62e-02	–
	48	2,208	1.09e-02	2.55	4.01e-03	2.82	4.24e-03	3.45
	384	15,936	1.58e-03	2.79	5.46e-04	2.88	4.40e-04	3.27
	3,072	120,576	2.15e-04	2.88	7.27e-05	2.91	4.98e-05	3.14
	24,576	936,960	2.84e-05	2.92	9.48e-06	2.94	5.85e-06	3.09
3	6	546	1.07e-02	–	4.02e-03	–	7.93e-03	–
	48	3,648	8.67e-04	3.63	2.90e-04	3.80	3.16e-04	4.65
	384	26,304	6.26e-05	3.79	2.01e-05	3.85	1.60e-05	4.30
	3,072	198,912	4.24e-06	3.89	1.35e-06	3.90	9.03e-07	4.15
	24,576	1,545,216	2.70e-07	3.97	8.52e-08	3.98	5.58e-08	4.02

Table 3: History of convergence of the error terms for the Example 4.1 ($\nu = 10^{-1}$).

k	N	η_1	order	η_2	order	η_3	order	η_4	order	η_5	order	eff
	6	1.06e-02	–	1.09e-01	–	4.27e-02	–	7.47e-02	–	4.26e-02	–	0.569
	48	2.63e-03	2.00	4.22e-02	1.37	1.71e-02	1.32	2.23e-02	1.75	1.44e-02	1.56	0.614
1	384	6.63e-04	1.99	1.19e-02	1.83	4.59e-03	1.89	6.08e-03	1.87	3.91e-03	1.89	0.600
	3072	1.73e-04	1.94	3.10e-03	1.94	1.14e-03	2.01	1.64e-03	1.89	1.00e-03	1.96	0.582
	24576	4.47e-05	1.95	7.85e-04	1.98	2.81e-04	2.02	4.30e-04	1.93	2.55e-04	1.98	0.569
	6	6.18e-03	–	3.78e-02	–	1.69e-02	–	2.28e-02	–	9.25e-03	–	0.579
	48	7.68e-04	3.01	6.43e-03	2.55	2.86e-03	2.56	3.46e-03	2.72	1.42e-03	2.70	0.648
2	384	1.01e-04	2.92	9.29e-04	2.79	4.05e-04	2.82	4.84e-04	2.84	1.96e-04	2.86	0.662
	3072	1.33e-05	2.93	1.26e-04	2.88	5.43e-05	2.90	6.54e-05	2.89	2.60e-05	2.92	0.665
	24576	1.71e-06	2.96	1.62e-05	2.96	8.40e-06	2.69	8.74e-06	2.90	3.31e-06	2.97	0.675
	6	1.31e-03	–	4.50e-03	–	1.71e-03	–	3.59e-03	–	6.72e-04	–	0.444
	48	8.11e-05	4.01	3.67e-04	3.62	1.40e-04	3.61	2.97e-04	3.59	5.80e-05	3.54	0.520
3	384	5.36e-06	3.92	2.65e-05	3.79	9.74e-06	3.85	2.13e-05	3.80	4.22e-06	3.78	0.533
	3072	3.51e-07	3.93	1.80e-06	3.88	6.43e-07	3.92	1.44e-06	3.89	2.86e-07	3.88	0.536
	24576	2.26e-08	3.96	1.16e-07	3.96	4.17e-08	3.95	9.52e-08	3.92	1.85e-08	3.95	0.549

Table 4: History of convergence of the terms composing the error estimator for the Example 4.1 ($\nu = 10^{-1}$).

k	N	N_{dof}	e_{L}	order	$\mathsf{e}_{\boldsymbol{u}}$	order	e_p	order
	6	168	1.24e-01	–	8.17e-02	–	2.97e-01	–
	48	1,128	6.00e-02	1.04	3.22e-02	1.35	8.46e-02	1.81
1	384	8,160	2.42e-02	1.31	1.02e-02	1.66	1.86e-02	2.18
	3,072	61,824	8.41e-03	1.52	3.19e-03	1.67	3.87e-03	2.27
	24,576	480,786	2.68e-03	1.65	9.85e-04	1.69	8.94e-04	2.11
	6	330	4.52e-02	–	3.29e-02	–	1.29e-01	–
	48	2,208	1.09e-02	2.05	5.27e-03	2.64	1.25e-02	3.36
2	384	15,936	2.04e-03	2.42	7.62e-04	2.79	1.18e-03	3.41
	3,072	120,576	3.49e-04	2.55	1.19e-04	2.68	1.26e-04	3.23
	24,576	936,960	5.49e-05	2.67	1.81e-05	2.71	1.49e-05	3.08
	6	546	1.11e-02	–	6.69e-03	–	2.81e-02	–
	48	3,648	1.10e-03	3.33	4.82e-04	3.79	9.26e-04	4.92
3	384	26,304	9.73e-05	3.50	3.44e-05	3.81	4.09e-05	4.50
	3,072	198,912	7.99e-06	3.61	2.63e-06	3.71	2.25e-06	4.19
	24,576	1,545,216	6.04e-07	3.73	1.94e-07	3.76	1.36e-07	4.04

Table 5: History of convergence of the error terms for the Example 4.1 ($\nu = 10^{-2}$).

k	N	η_1	order	η_2	order	η_3	order	η_4	order	η_5	order	eff
	6	1.32e-03	–	1.24e-01	–	5.60e-02	–	3.60e-02	–	1.58e-02	–	0.425
	48	3.68e-04	1.85	6.77e-02	0.87	3.12e-02	0.84	1.40e-02	1.36	8.09e-03	0.96	0.703
1	384	7.56e-05	2.28	2.32e-02	1.54	1.04e-02	1.59	3.09e-03	2.18	2.84e-03	1.51	0.800
	3,072	1.51e-05	2.32	7.08e-03	1.71	2.74e-03	1.92	6.67e-04	2.21	8.53e-04	1.73	0.783
	24,576	3.36e-06	2.17	2.14e-03	1.72	9.55e-04	1.52	1.61e-04	2.05	2.43e-04	1.81	0.790
	6	7.35e-04	–	6.69e-02	–	2.64e-02	–	1.48e-02	–	4.94e-03	–	0.524
	48	7.38e-05	3.32	1.63e-02	2.04	7.26e-03	1.86	2.07e-03	2.84	1.09e-03	2.17	1.031
2	384	7.70e-06	3.26	3.12e-03	2.38	1.37e-03	2.41	2.30e-04	3.17	1.98e-04	2.47	1.382
	3,072	9.22e-07	3.06	5.38e-04	2.54	2.30e-04	2.57	2.66e-05	3.11	3.34e-05	2.57	1.506
	24,576	1.21e-07	2.92	8.47e-05	2.67	3.58e-05	2.68	3.37e-06	2.98	5.19e-06	2.68	1.545
	6	1.66e-04	–	1.53e-02	–	6.62e-03	–	2.61e-03	–	8.04e-04	–	0.547
	48	6.78e-06	4.61	1.38e-03	3.47	6.21e-04	3.41	1.51e-04	4.11	7.00e-05	3.52	1.004
3	384	3.68e-07	4.20	1.21e-04	3.52	5.22e-05	3.57	9.21e-06	4.04	6.20e-06	3.50	1.189
	3,072	2.36e-08	3.96	1.01e-05	3.58	4.06e-06	3.69	5.92e-07	3.96	5.17e-07	3.58	1.251
	24,576	1.61e-09	3.87	7.76e-07	3.70	2.93e-07	3.79	3.96e-08	3.90	3.95e-08	3.71	1.282

Table 6: History of convergence of the terms composing the error estimator for the Example 4.1 ($\nu = 10^{-2}$).

4.2. A low regularity solution

Based on a numerical experiment presented in [8], we set $\Omega =]-1,1[\times]-1,1[\times]0,1[\setminus]0,1[\times]-1,0[\times]0,1[$, $\nu = 1$ and $\boldsymbol{\beta} = (1,-1,0)$. The source term $\boldsymbol{f}$ and the boundary data $\boldsymbol{u}_D$ are chosen such that the exact solution of the problem is given by $p(x_1,x_2,x_3) := 0$ and $\boldsymbol{u} := \left(\frac{\partial S}{\partial x_1}, \frac{\partial S}{\partial x_2}, 0\right)$, where S is given, in cylindrical coordinates, by $S(r,\phi) = r^{\frac{4}{3}} \sin\left(\frac{4}{3}\phi\right)$. We note that $\boldsymbol{u} \in H^{\frac{4}{3}-\epsilon}(\Omega)^3$, $\epsilon > 0$, due to a singularity located at x_3-axis. In Figure 1, we present the orders of convergence for e_h using uniform and adaptive refinements, $\theta = 0.25$, for $k = 1$.

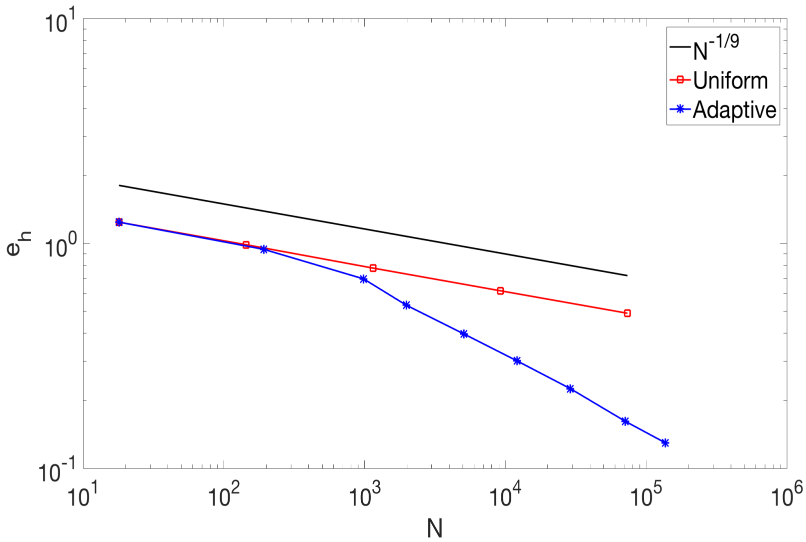

Figure 1: History of convergence for e_h with uniform and adaptive ($\theta = 0.25$) refinement, for $k = 1$, in the low regularity example.

We observe that the uniform refinement strategy provides an approximate solution that converges with the predicted order of convergence, $\mathcal{O}(h^{1/3})$, because the singularity of the velocity while the adaptive scheme let us achieve a better order of convergence and lower error magnitudes than the uniform case.

In Figure 2 we show the final adaptively refined mesh and how the mesh is locally refined near the corner line $x_1 = x_2 = 0$, where the gradient of the velocity has a singularity. We also show the isovalues of the velocity magnitude.

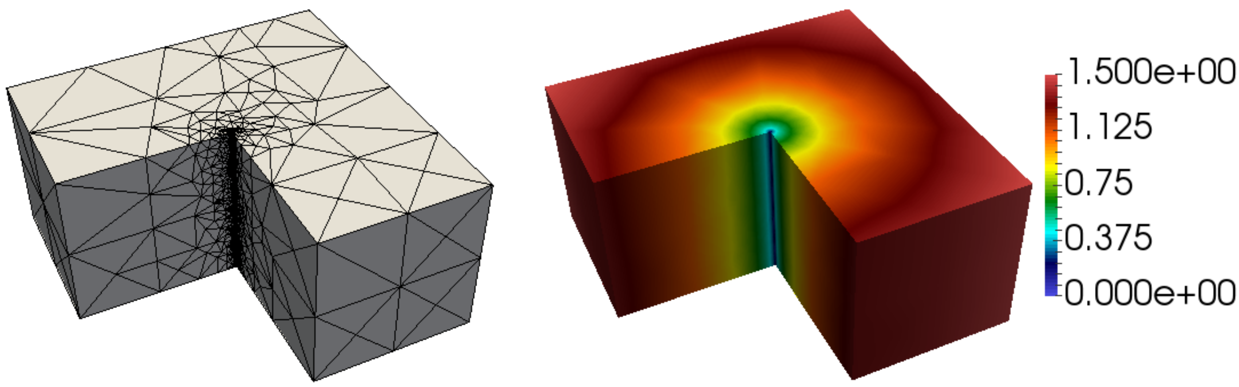

Figure 2: Final adaptive mesh (12,114 elements, $\theta = 0.25$) refinement ($k = 1$) and corresponding isovalues of the velocity magnitude, for the low regularity solution.

4.3. The lid-driven cavity problem

For this test, we consider $\Omega =]0,1[^3$ and set $\nu = 1$, $\boldsymbol{\beta} = (1,0,0)$, $\boldsymbol{f} = \boldsymbol{0}$ and $\boldsymbol{u}_D = (1,0,0)$, on $x_2 = 1$, and $\boldsymbol{0}$ on the rest of the boundary of Ω. Note that boundary layers arise at the edges of the top face of the domain, due to the discontinuities on the boundary condition. This fact is captured by our estimator by refining mainly in those edges as can be seen in Figure 3, where the initial and an adapted ($\theta = 0.25$) meshes are displayed. Figure 4 shows a cross-section at $z = 0.5$ of the same adapted mesh and the isovalues of the first component of the velocity.

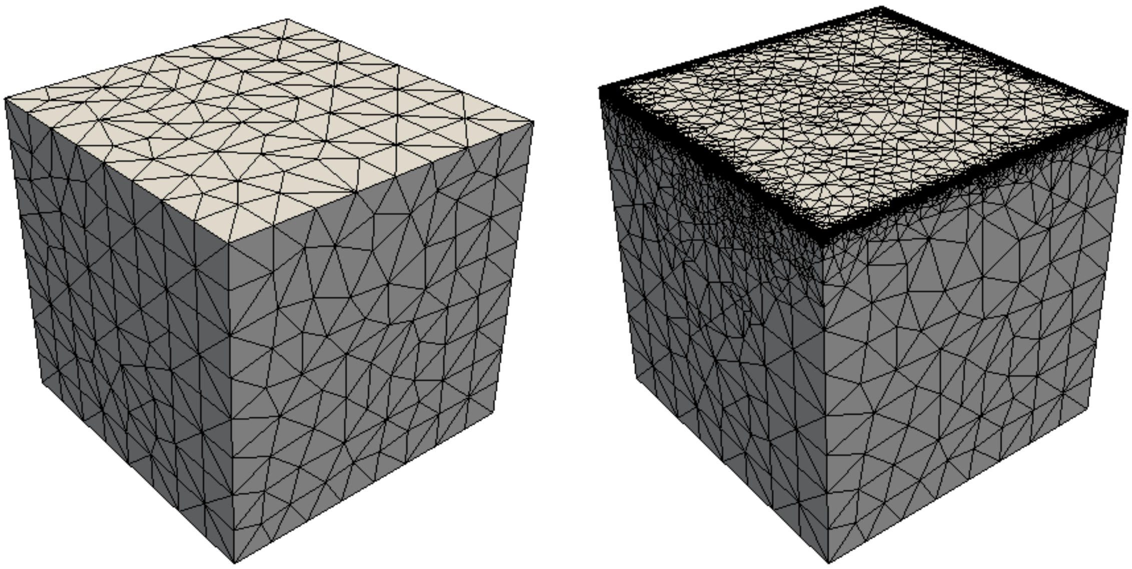

Figure 3: Initial mesh (2,255 elements) and final adapted mesh (270,941 elements) for the cavity problem ($k = 1$, $\theta = 0.25$).

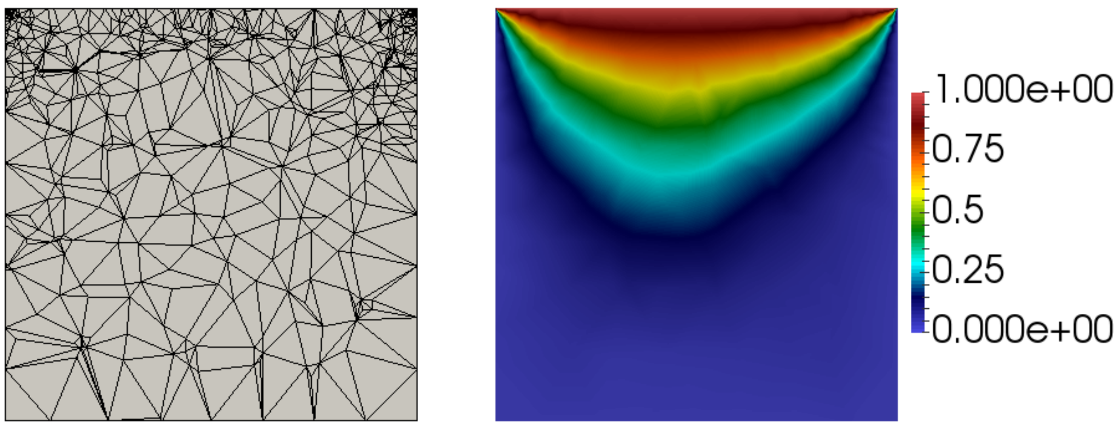

Figure 4: A vertical cut at $z = 0.5$ of the adapted mesh (270,941 elements, left) and the isovalues of the first component of the velocity in this mesh (right) at this cut ($k = 1$, $\theta = 0.01$).

4.4. An application to steady-state incompressible Navier–Stokes equations

As we said in the introduction, one of our motivations is to apply the proposed *a posteriori* error estimator to the Navier–Stokes equations, whose solution was constructed using a sequence on Oseen equations associated to a Picard's iteration. We consider $\Omega =]0,1[^3$ and choose the data $\boldsymbol{f}$ and $\boldsymbol{u}_D$ so that the exact solution is given by

$$\boldsymbol{u}(x_1, x_2, x_3) := (\exp(x_1)\sin(x_3), -\exp(x_1)\sin(x_3), \exp(x_1)\cos(x_3) - \exp(x_1)\cos(x_2))$$

and

$$p(x_1, x_2, x_3) := (1/2)\exp(2x_1) + (1/4)(\exp(2) - 1).$$

We set $\nu = 1$ and consider the following algorithm to solve the incompressible Navier–Stokes equations:

(i) Solve $\mathrm{HDG}_{Oseen}(\mathbf{0})$ and set $\boldsymbol{\beta}_1 := \boldsymbol{u}_h^{*,0}$, where $\boldsymbol{u}_h^{*,0}$ is the postprocessed velocity (2.5) constructed by using the solution of $\mathrm{HDG}_{Oseen}(\mathbf{0})$.

(ii) For $i = 1, \ldots, I_{\max}$, if $\|\boldsymbol{u}_h^{*,i} - \boldsymbol{u}_h^{*,i-1}\| < \text{tol}$, solve $\mathrm{HDG}_{Oseen}(\boldsymbol{\beta}_i)$ and set $\boldsymbol{\beta}_{i+1} := \boldsymbol{u}_h^{*,i}$, where $\boldsymbol{u}_h^{*,i}$ is the postprocessed velocity (2.5) constructed by using the solution of $\mathrm{HDG}_{Oseen}(\boldsymbol{\beta}_i)$.

Here, $\mathrm{HDG}_{Oseen}(\boldsymbol{\beta})$ is the HDG formulation with data $\boldsymbol{f}$, $\boldsymbol{u}_D$ and convective velocity $\boldsymbol{\beta}$; tol is the tolerance associated to the stopping criteria, $\|\cdot\|$ the Euclidean norm and $I_{\max}$ the maximum number of iterations. Let be $\boldsymbol{u}_h^{*,NS}$ the postprocessed velocity and L_h^{NS}, p_h^{NS} the solution of the Navier–Stokes equations obtained in (ii). Then, we will use L_h^{NS}, $\boldsymbol{u}_h^{*,NS}$, p_h^{NS} and $\boldsymbol{\beta} = \boldsymbol{u}_h^{*,NS}$ to compute our *a posteriori* error estimator for the error with respect to the solution $(\mathrm{L}_h^{NS}, \boldsymbol{u}_h^{*,NS}, p_h^{NS})$.

k	N	N_{sist}	e_{L}	order	$\mathsf{e}_{\boldsymbol{u}}$	order	e_p	order	iter
	6	168	$6.02E-01$	–	$2.10E-01$	–	$1.80E-01$	–	3
	48	1,128	$1.96E-01$	1.62	$6.35E-02$	1.73	$5.24E-02$	1.78	3
1	384	8,160	$5.60E-02$	1.81	$1.77E-02$	1.84	$1.29E-02$	2.02	3
	3,072	61,824	$1.49E-02$	1.91	$4.68E-03$	1.92	$3.18E-03$	2.03	4
	24,576	480,786	$3.84E-03$	1.96	$1.21E-03$	1.96	$7.89E-04$	2.01	4
	6	330	$7.83E-02$	–	$2.64E-02$	–	$2.77E-02$	–	3
	48	2,208	$1.33E-02$	2.56	$4.03E-03$	2.71	$3.79E-03$	2.87	3
2	384	15,936	$1.89E-03$	2.81	$5.51E-04$	2.87	$4.80E-04$	2.98	3
	3,072	120,576	$2.51E-04$	2.92	$7.18E-05$	2.94	$5.97E-05$	3.01	4
	24,576	936,960	$3.22E-05$	2.96	$9.17E-06$	2.97	$7.40E-06$	3.01	4
	6	546	$8.09E-03$	–	$2.59E-03$	–	$3.15E-03$	–	3
	48	3,648	$7.11E-04$	3.51	$2.05E-04$	3.66	$2.22E-04$	3.83	3
3	384	26,304	$5.09E-05$	3.80	$1.43E-05$	3.84	$1.43E-05$	3.96	3
	3,072	198,912	$3.31E-06$	3.94	$9.37E-07$	3.94	$8.97E-07$	3.99	4
	24,576	1,545,216	$2.15E-07$	3.97	$6.12E-08$	3.95	$5.62E-08$	3.99	4

Table 7: History of convergence of the error terms for the Example 4.4.

k	N	η_1	order	η_2	order	η_3	order	η_4	order	η_5	order	eff
	6	$7.21E-01$	–	$9.90E-02$	–	$4.20E-02$	–	$1.03E+00$	–	$1.33E-01$	–	1.915
	48	$2.02E-01$	1.83	$3.73E-02$	1.41	$1.74E-02$	1.27	$3.69E-01$	1.48	$4.27E-02$	1.64	1.998
1	384	$5.24E-02$	1.95	$1.10E-02$	1.77	$5.01E-03$	1.79	$1.06E-01$	1.80	$1.21E-02$	1.82	1.991
	3,072	$1.32E-02$	1.99	$2.92E-03$	1.91	$1.31E-03$	1.93	$2.83E-02$	1.91	$3.20E-03$	1.92	1.979
	24,576	$3.32E-03$	2.00	$7.51E-04$	1.96	$3.34E-04$	1.98	$7.28E-03$	1.96	$8.21E-04$	1.96	1.972
	6	$1.72E-01$	–	$1.87E-02$	–	$8.14E-03$	–	$1.71E-01$	–	$1.33E-02$	–	2.794
	48	$2.45E-02$	2.81	$3.24E-03$	2.52	$1.66E-03$	2.30	$3.11E-02$	2.46	$1.99E-03$	2.75	2.763
2	384	$3.17E-03$	2.95	$4.67E-04$	2.79	$2.48E-04$	2.74	$4.60E-03$	2.76	$2.68E-04$	2.89	2.767
	3,072	$4.00E-04$	2.99	$6.23E-05$	2.91	$3.36E-05$	2.89	$6.24E-04$	2.88	$3.48E-05$	2.95	2.784
	24,576	$5.02E-05$	3.00	$8.01E-06$	2.96	$4.37E-06$	2.94	$8.13E-05$	2.94	$4.42E-06$	2.97	2.798
	6	$2.82E-02$	–	$2.14E-03$	–	$9.76E-04$	–	$2.06E-02$	–	$1.01E-03$	–	3.860
	48	$2.03E-03$	3.80	$1.84E-04$	3.55	$9.63E-05$	3.34	$1.84E-03$	3.48	$7.66E-05$	3.72	3.554
3	384	$1.32E-04$	3.94	$1.30E-05$	3.82	$7.08E-06$	3.76	$1.29E-04$	3.83	$5.19E-06$	3.88	3.379
	3,072	$8.31E-06$	3.99	$8.33E-07$	3.97	$4.55E-07$	3.96	$8.31E-06$	3.96	$3.33E-07$	3.96	3.320
	24,576	$5.21E-07$	4.00	$5.30E-08$	4.01	$2.93E-08$	4.00	$5.31E-07$	3.99	$2.12E-08$	3.98	3.240

Table 8: History of convergence of the terms composing the error estimator for the Example 4.4.

Table 7 shows the history of convergence of the error of each variable with all the error terms converging with optimal order of $k+1$, exactly as predicted in [6] . In addition, we display the number of iterations, iter, needed to get the solution of Navier–Stokes equations. In Table 8, we see that each term of the error estimator converge with order $k+1$ and, as for Oseen equations, the effectivity index remains bounded.

Acknowledgements

R. Araya and M. Solano were partially supported by CONICYT-Chile through grants FONDECYT-1150174, FONDECYT-1160320 and project AFB170001 of the PIA Program: Concurso Apoyo a Centros Científicos y Tecnológicos de Excelencia con Financiamiento Basal. P. Vega was partially supported by CONICYT-Chile through scholarship PCHA/Doctorado Nacional/2014-21140137 and project AFB170001 of the PIA Program: Concurso Apoyo a Centros Científicos y Tecnológicos de Excelencia con Financiamiento Basal.

References

[1] Ainsworth, M., Fu, G., 2018. Fully computable *a posteriori* error bounds for hybridizable discontinuous Galerkin finite element approximations. J. Sci. Comput. 77, 443–466.

[2] Araya, R., Solano, M., Vega, P., 2018. Analysis of an adaptive HDG method for the Brinkman problem. IMA J. Numer. Anal., dry031.

[3] Ayuso, B., Marini, L. D., 2009. Discontinuous Galerkin methods for advection-diffusion-reaction problems. SIAM J. Numer. Anal. 47, 1391–1420.

[4] Bustinza, R., Lombardi, A., Solano, M., 2016. An anisotropic *a priori* error estimate for a convection-dominated diffusion problem using the HDG method. Preprint 2016-38, Centro de Investigación en Ingeniería Matemática (CI^2MA), Universidad de Concepción, Chile.

[5] Cesmelioglu, A., Cockburn, B., Nguyen, N. C., Peraire, J., 2013. Analysis of HDG methods for Oseen equations. J. Sci. Comput. 55, 392–431.

[6] Cesmelioglu, A., Cockburn, B., Qiu, W., 2017. Analysis of a hybridizable discontinuous Galerkin method for the steady-state incompressible Navier–Stokes equations. Math. Comp. 86, 1643–1670.

[7] Chen, H., Li, J., Qiu, W., 2016. Robust a posteriori error estimates for HDG method for convection–diffusion equations. IMA J. Numer. Anal. 36, 437–462.

[8] Chen, H., Qiu, W., Shi, K., 2018. A priori and computable a posteriori error estimates for an HDG method for the coercive Maxwell equations. Comput. Methods in Appl. Mech. Engrg 333, 287 – 310.

[9] Chen, Y., Cockburn, B., 2012. Analysis of variable-degree HDG methods for convection-diffusion equations. Part I: general nonconforming meshes. IMA J. Numer. Anal. 32, 1267–1293.

[10] Chen, Y., Cockburn, B., 2014. Analysis of variable-degree HDG methods for convection-diffusion equations. Part II: Semimatching nonconforming meshes. Math. Comp. 83, 87–111.

[11] Clément, P., 1975. Approximation by finite element functions using local regularization. Rev. Française Automat. Informat. Recherche Opérationnelle Sér. 9, 77–84.

[12] Cockburn, B., Dong, B., Guzmán, J., Restelli, M., Sacco, R., 2009. A hybridizable discontinuous Galerkin method for steady-state convection-diffusion-reaction problems. SIAM J. Sci. Comput. 31, 3827–3846.

[13] Cockburn, B., Gopalakrishnan, J., 2009. The derivation of hybridizable discontinuous Galerkin methods for Stokes flow. SIAM J. Numer. Anal. 47, 1092–1125.

[14] Cockburn, B., Gopalakrishnan, J., Lazarov, R. D., 2009. Unified hybridization of discontinuous Galerkin, mixed, and continuous Galerkin methods for second order elliptic problems. SIAM J. Numer. Anal. 47, 1319–1365.

[15] Cockburn, B., Gopalakrishnan, J., Nguyen, N. C., Peraire, J., Sayas, F.-J., 2011. Analysis of HDG methods for Stokes flow. Math. Comp. 80, 723–760.

[16] Cockburn, B., Sayas, F.-J., 2014. Divergence-conforming HDG methods for Stokes flows. Math. Comp. 83, 1571–1598.

[17] Cockburn, B., Zhang, W., 2012. A posteriori error estimates for HDG methods. J. Sci. Comput. 51, 582–607.

[18] Cockburn, B., Zhang, W., 2013. A posteriori error analysis for hybridizable discontinuous Galerkin methods for second order elliptic problems. SIAM J. Numer. Anal. 51, 676–693.

[19] Cockburn, B., Zhang, W., 2014. An a posteriori error estimate for the variable-degree Raviart-Thomas method. Math. Comp. 83, 1063–1082.

[20] Di Pietro, D. A., Ern, A., 2012. Mathematical aspects of discontinuous Galerkin methods. Vol. 69 of Mathématiques & Applications. Springer–Verlag, Berlin–Heilderber.

[21] Fu, G., Jin, Y., Qiu, W., 2018. Parameter-free superconvergent H(div)-conforming HDG methods for the Brinkman equations. IMA Journal of Numerical Analysis, dry001.

[22] Fu, G., Qiu, W., Zhang, W., 2015. An analysis of HDG methods for convection–dominated diffusion problems. ESAIM: M2AN 49, 225–256.

[23] Fu, Z., Gatica, L. F., Sayas, F.-J., 2015. Algorithm 949: Matlab tools for HDG in three dimensions. ACM Trans. Math. Softw. 41, 20:1–20:21.

[24] Fung, Y. C., 1996. Biomechanics: Circulation. Plant Gene Research: Basic Knowledge. Springer New York.
[25] Gatica, G. N., Sequeira, F. A., Dec 2015. Analysis of an augmented HDG method for a class of quasi–Newtonian Stokes flows. J. Sci. Comput. 65, 1270–1308.
[26] Gatica, G. N., Sequeira, F. A., 2016. A priori and a posteriori error analyses of an augmented HDG method for a class of quasi-Newtonian Stokes flows. J. Sci. Comput. 69, 1192–1250.
[27] Gatica, G. N., Sequeira, F. A., 2017. Analysis of the HDG method for the Stokes–Darcy coupling. Numer. Methods Partial Differential Equations 33, 885–917.
[28] Gatica, L. F., Sequeira, F. A., 2018. A priori and a posteriori error analyses of an HDG method for the Brinkman problem. Comput. Math. Appl. 75, 1191–1212.
[29] Giorgiani, G., Fernández-Méndez, S., Huerta, A., 2014. Hybridizable discontinuous Galerkin with degree adaptivity for the incompressible Navier–Stokes equations. Comput. & Fluids 98, 196–208.
[30] Girault, V., Raviart, P.-A., 1986. Finite element methods for Navier-Stokes equations. Theory and algorithms. Vol. 5 of Springer Series in Computational Mathematics. Springer-Verlag, Berlin.
[31] Jin, Y., 2016. Local analysis of HDG methods for convection-dominated diffusion problems. J. Comput. Appl. Math. 304, 57–72.
[32] Karakashian, O. A., Pascal, F., 2003. A posteriori error estimates for a discontinuous Galerkin approximation of second-order elliptic problems. SIAM J. Numer. Anal. 41, 2374–2399.
[33] Nguyen, N. C., Peraire, J., Cockburn, B., 2009. An implicit high–order hybridizable discontinuous Galerkin method for linear convection–diffusion equations. J. Comput. Phys. 228, 3232–3254.
[34] Nguyen, N. C., Peraire, J., Cockburn, B., 2009. An implicit high–order hybridizable discontinuous Galerkin method for nonlinear convection–diffusion equations. J. Comput. Phys. 228, 8841–8855.
[35] Nguyen, N. C., Peraire, J., Cockburn, B., 2010. A hybridizable discontinuous Galerkin method for Stokes flow. Comput. Methods Appl. Mech. Engrg. 199, 582–597.
[36] Nguyen, N. C., Peraire, J., Cockburn, B., 2011. An implicit high-order hybridizable discontinuous Galerkin method for the incompressible Navier–Stokes equations. J. Comput. Phys. 230, 1147–1170.
[37] Oseen, C. W., 1910. Über die Stoke'sche Formel und über eine verwandte Aufgabe in der Hydrodynamik. Arkiv för matematik, astronomi och fysik. Almqvist & Wiksell.
[38] Peraire, J., Nguyen, N. C., Cockburn, B., 2010. A hybridizable discontinuous Galerkin method for the compressible Euler and Navier–Stokes equations. In: 48th AIAA Aerospace Sciences Meeting Including the New Horizons Forum and Aerospace Exposition.
[39] Peraire, J., Nguyen, N. C., Cockburn, B., 2010. A hybridizable discontinuous Galerkin method for the incompressible Euler and Navier–Stokes equations. In: 48th AIAA Aerospace Sciences Meeting Including the New Horizons Forum and Aerospace Exposition.
[40] Qiu, W., Shi, K., 2016. An HDG method for convection diffusion equation. J. Sci. Comput. 66, 346–357.
[41] Qiu, W., Shi, K., 2016. A superconvergent HDG method for the incompressible Navier–Stokes equations on general polyhedral meshes. IMA J. Numer. Anal. 36, 1943–1967.
[42] Rhebergen, S., Wells, G. N., 2018. A Hybridizable Discontinuous Galerkin Method for the Navier–Stokes Equations with Pointwise Divergence-Free Velocity Field. J. Sci. Comput. 76, 1484–1501.
[43] Si, H., 2015. Tetgen, a Delaunay-based quality tetrahedral mesh generator. ACM Trans. Math. Softw. 41, 11:1–11:36.
[44] Verfürth, R., 1998. A posteriori error estimators for convection–diffusion equations. Numer. Math. 80, 641–663.